Magnetic Particle Imaging

Vít Herynek

Center for Advanced Preclinical Imaging (CAPI)

1. LF UK

www.capi.lf1.cuni.cz

Magnetic Particle Imaging

- Novel tomographic method, uses magnetic fields
- No ionizing radiation, non-invasive imaging
- **Requires a tracer!**
- No native imaging, no anatomical information
- Requires colocalization with another imaging methods (X-Ray, MRI, CT, optical…)

Tracer – **superparamagnetic particles**

History

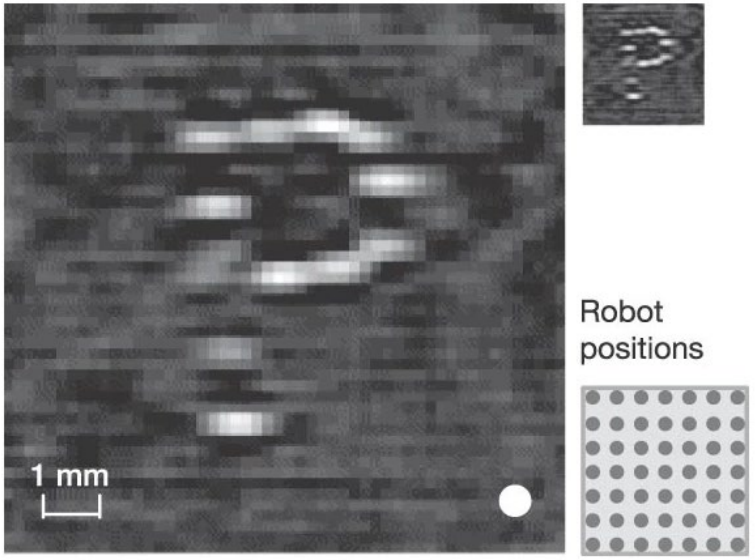

2001 – first MPI image

2005 – Gleich B, Weizenecker J. Tomographic imaging using nonlinear response of magnetic particles. Nature 2005; 435:1214-1217

2008 – Gleich B, Weizenecker J, Borgert J. Experimental results on fast 2D-encoded magnetic particle imaging. Physics in Medicine and Biology 2008;53:N81-N84

A small detour…

Paramagnetism
Ferromagnetism
Superparamagnetism

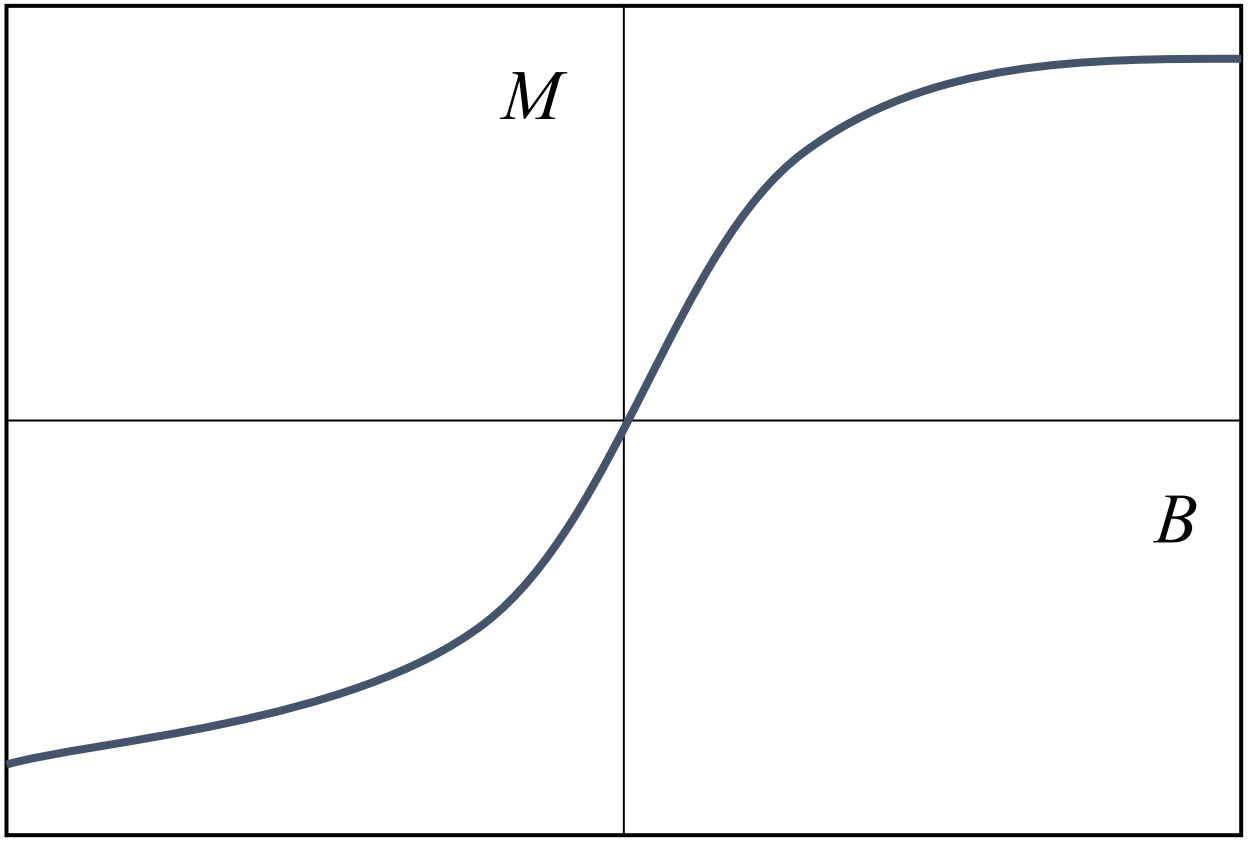

Paramagnetism

$B = 0, M = 0$

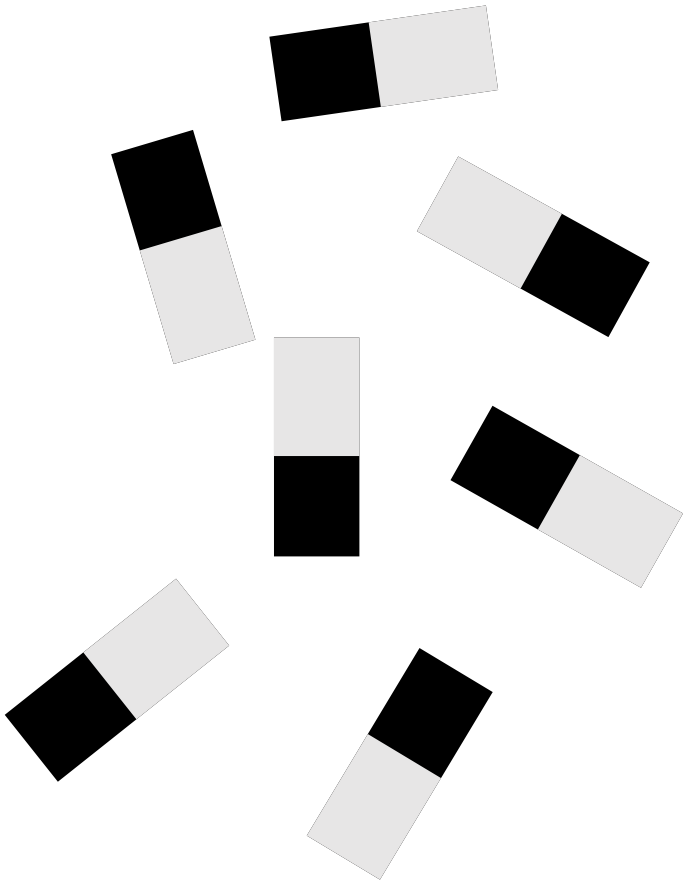

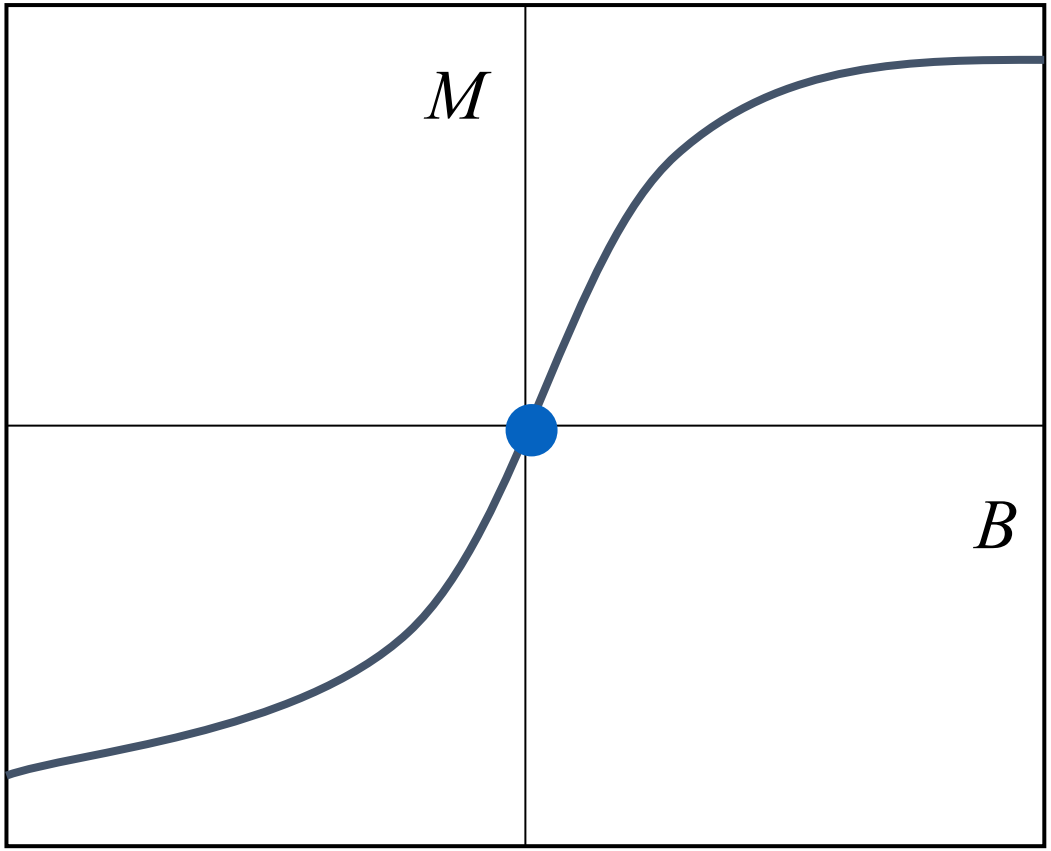

Paramagnetism

$B \neq 0, M \neq 0$

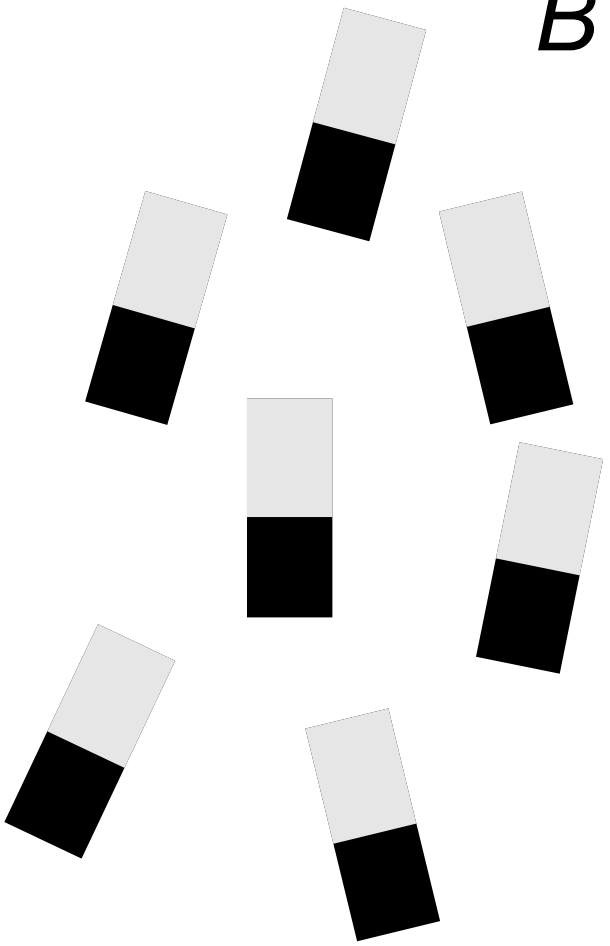

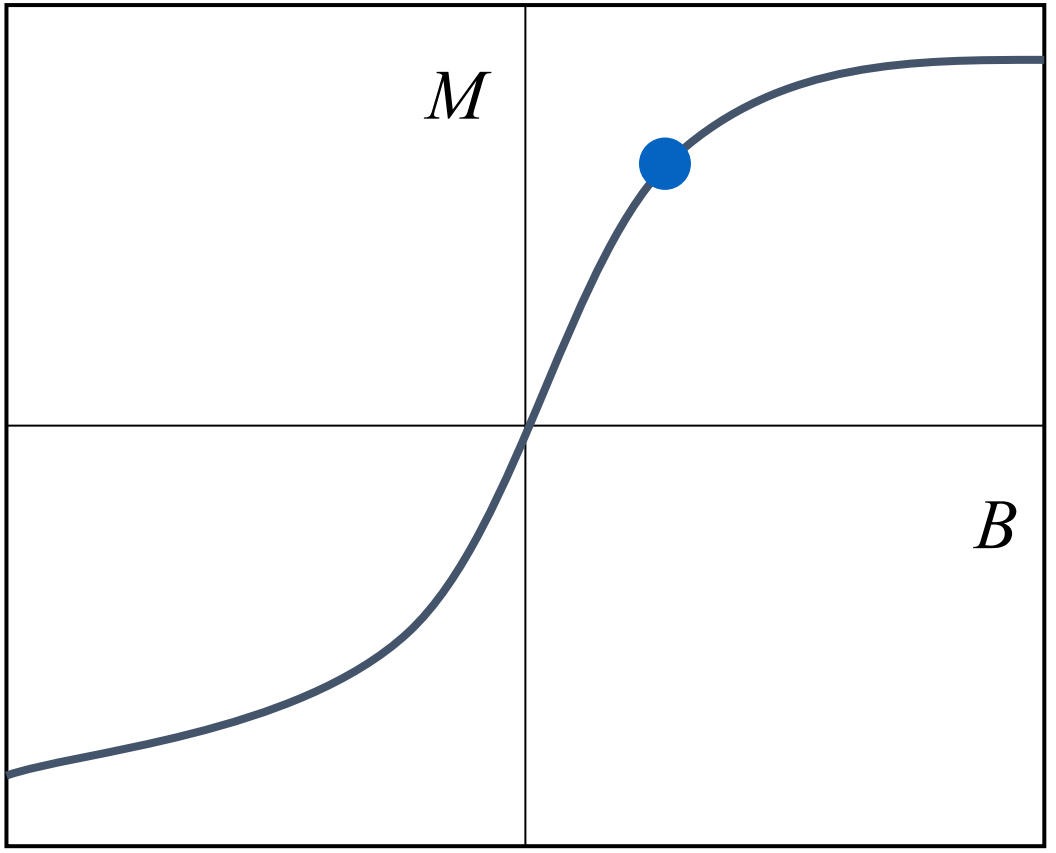

Paramagnetism

$B \neq 0, M \neq 0$

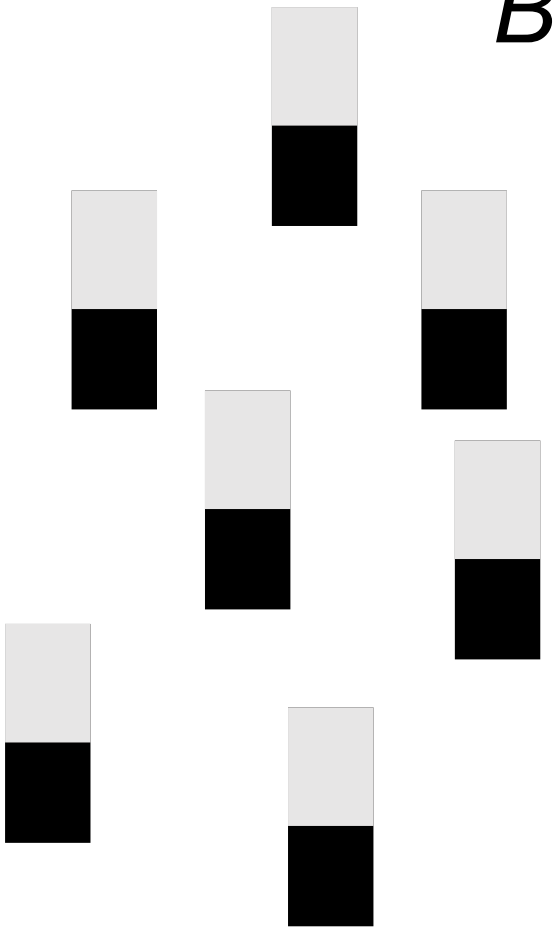

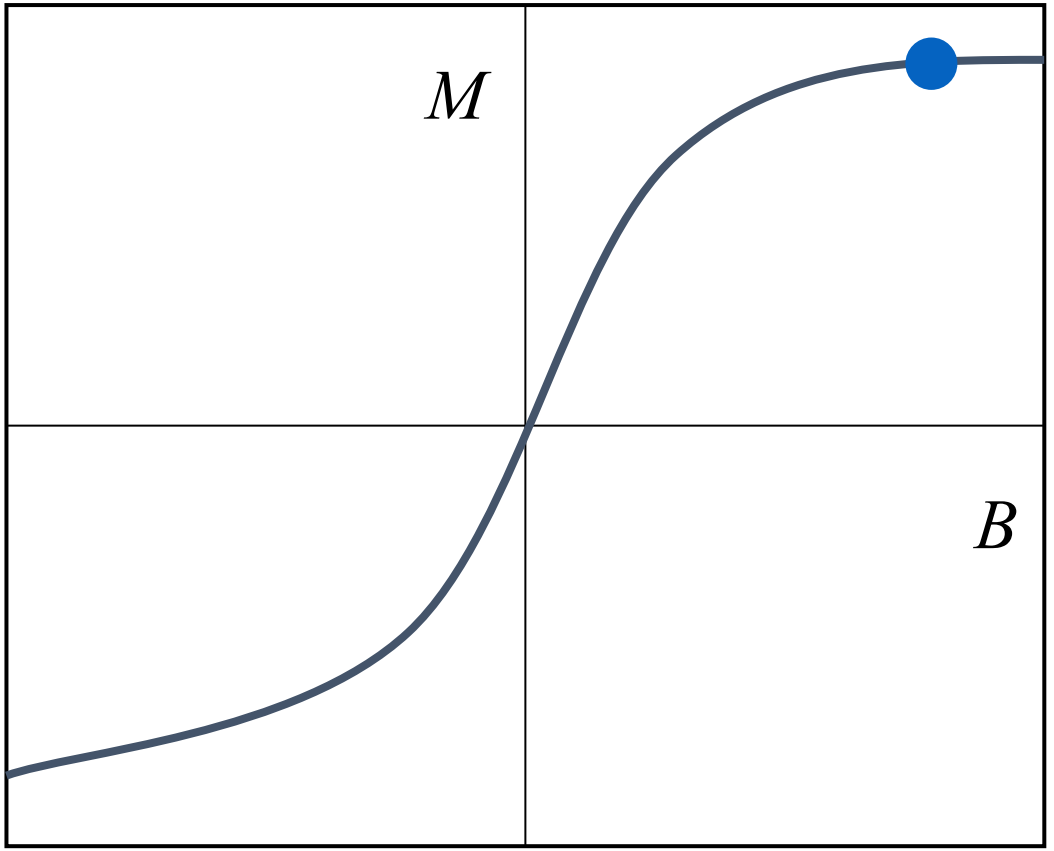

Paramagnetism

$B = 0, M = 0$

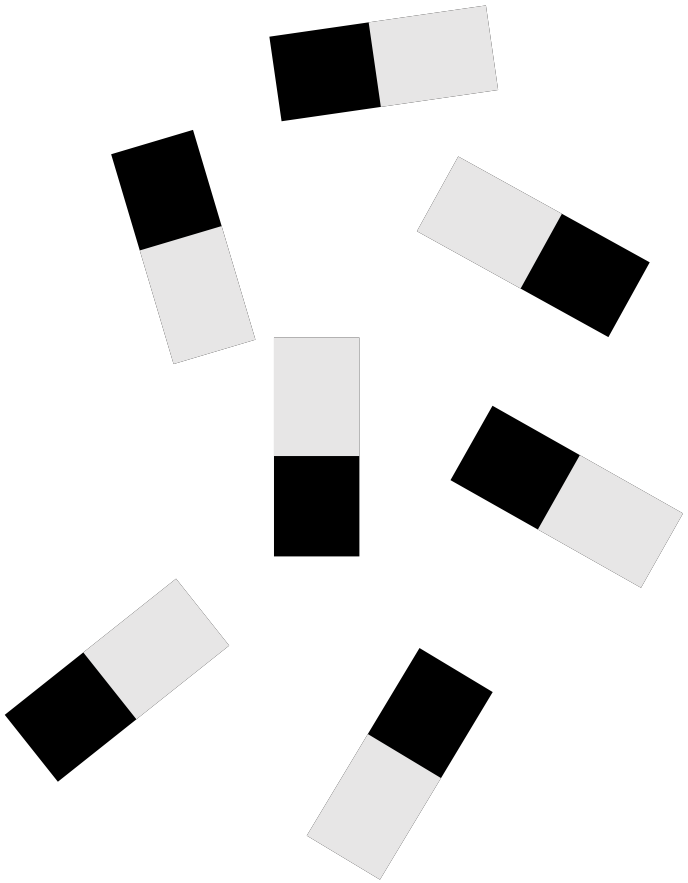

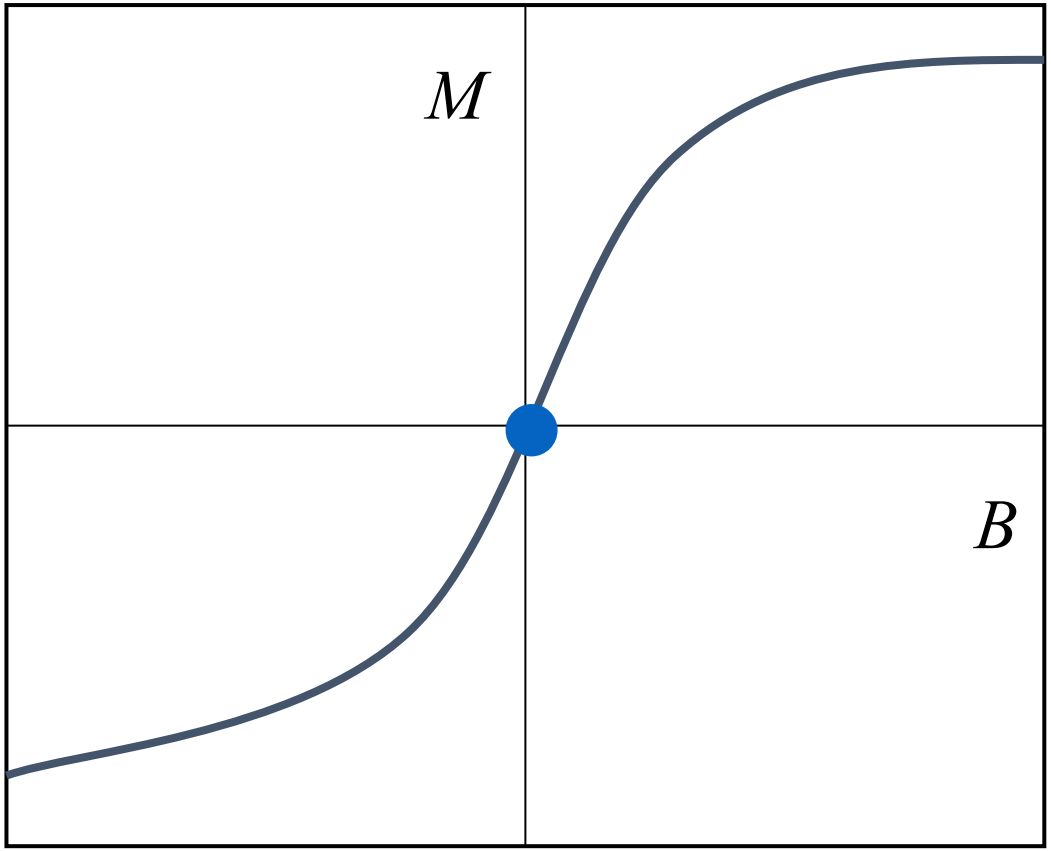

Ferromagnetism

$B = 0,\ M \neq 0$

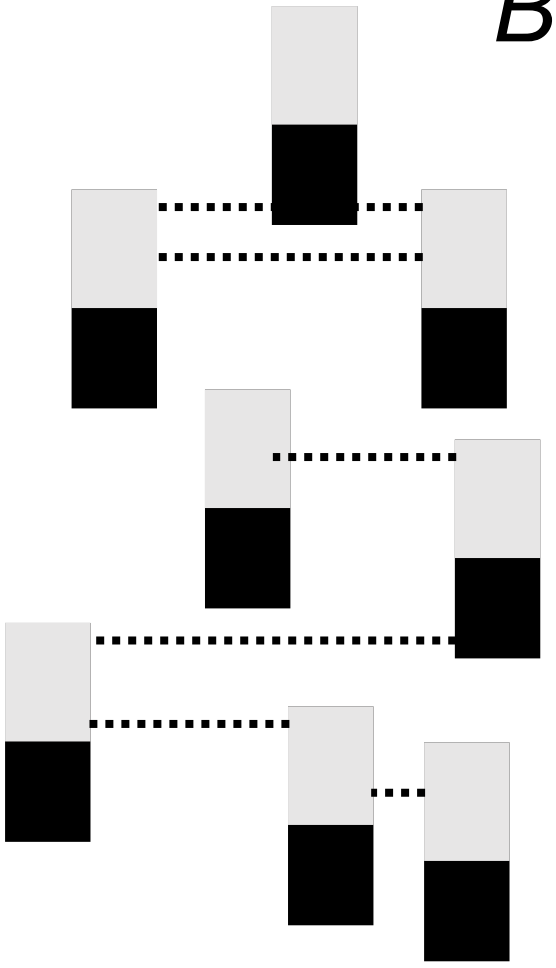

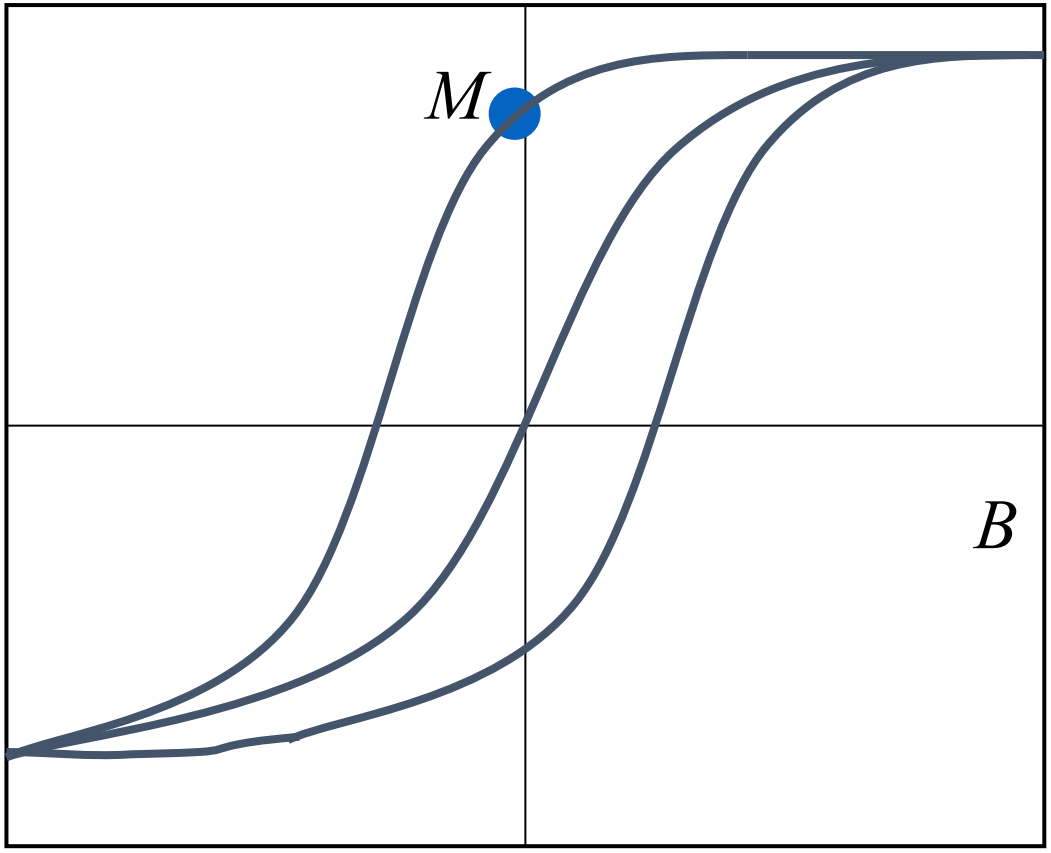

Ferromagnetism → Changes to paramagnetism above Currie temperature

$B = 0, M = 0$

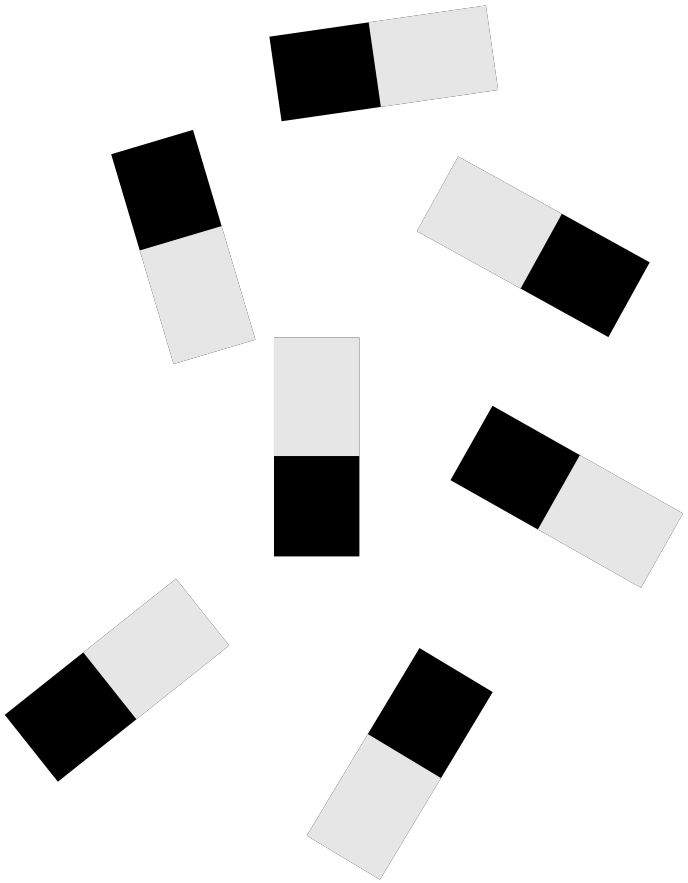

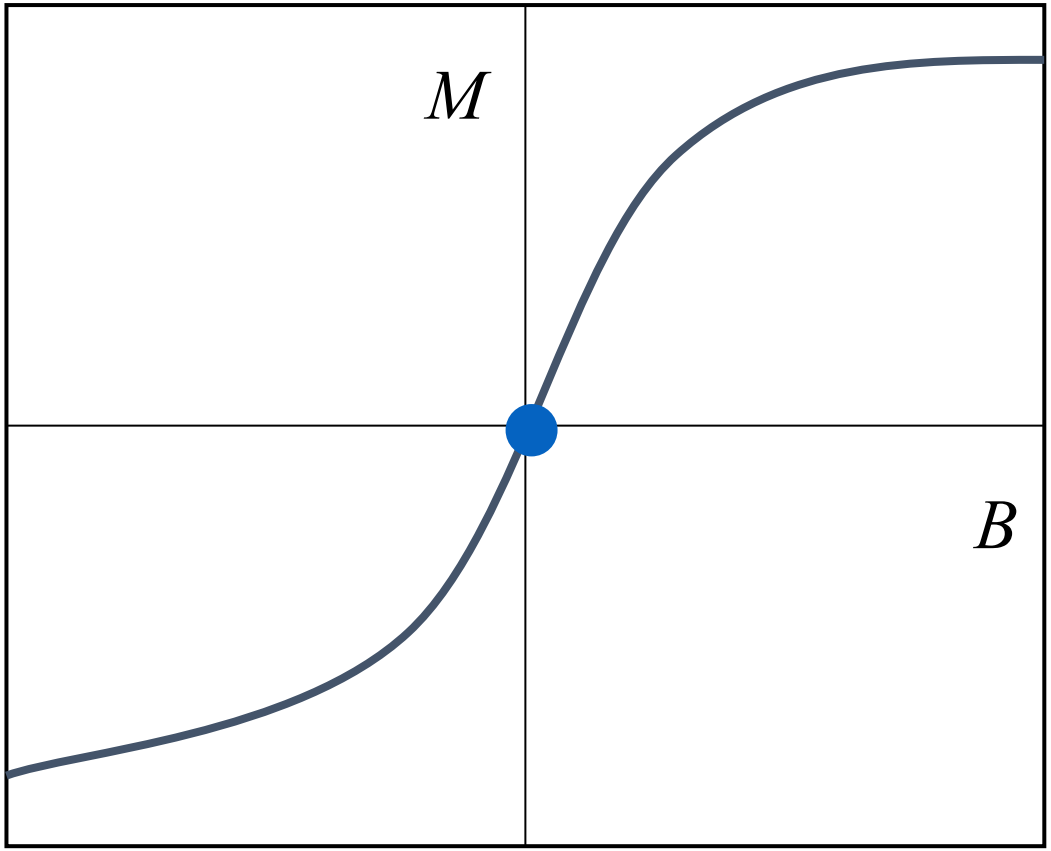

Superparamagnetism

$B = 0, M = 0$

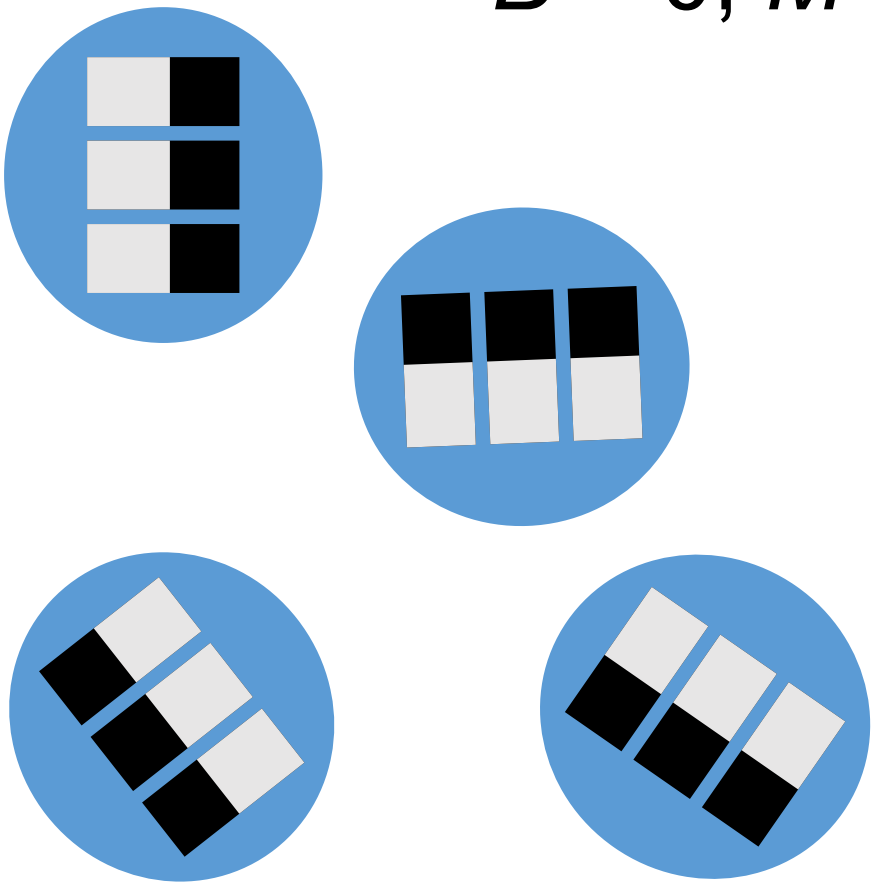

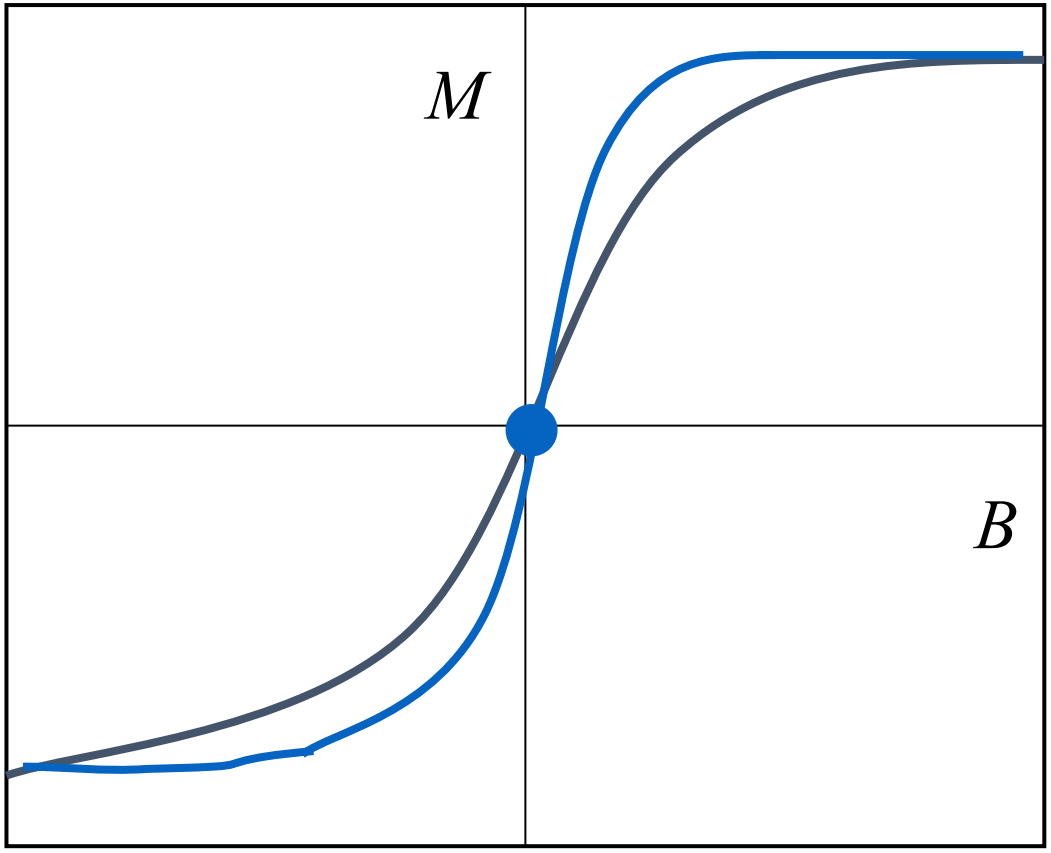

Superparamagnetism

$B \neq 0, M \neq 0$

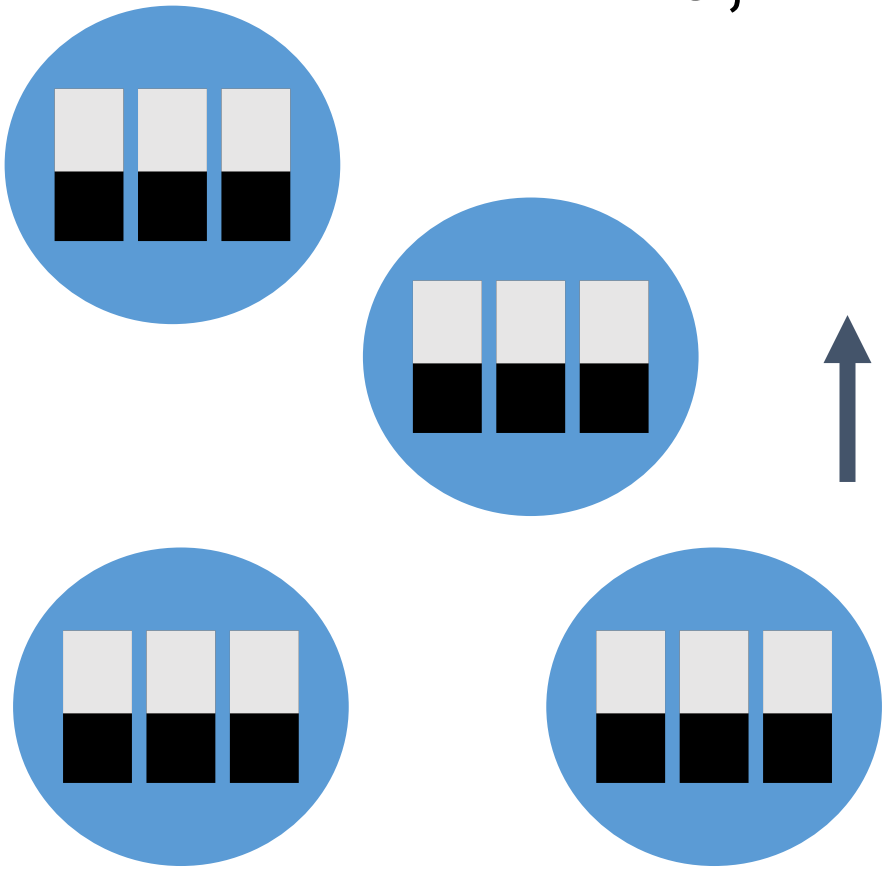

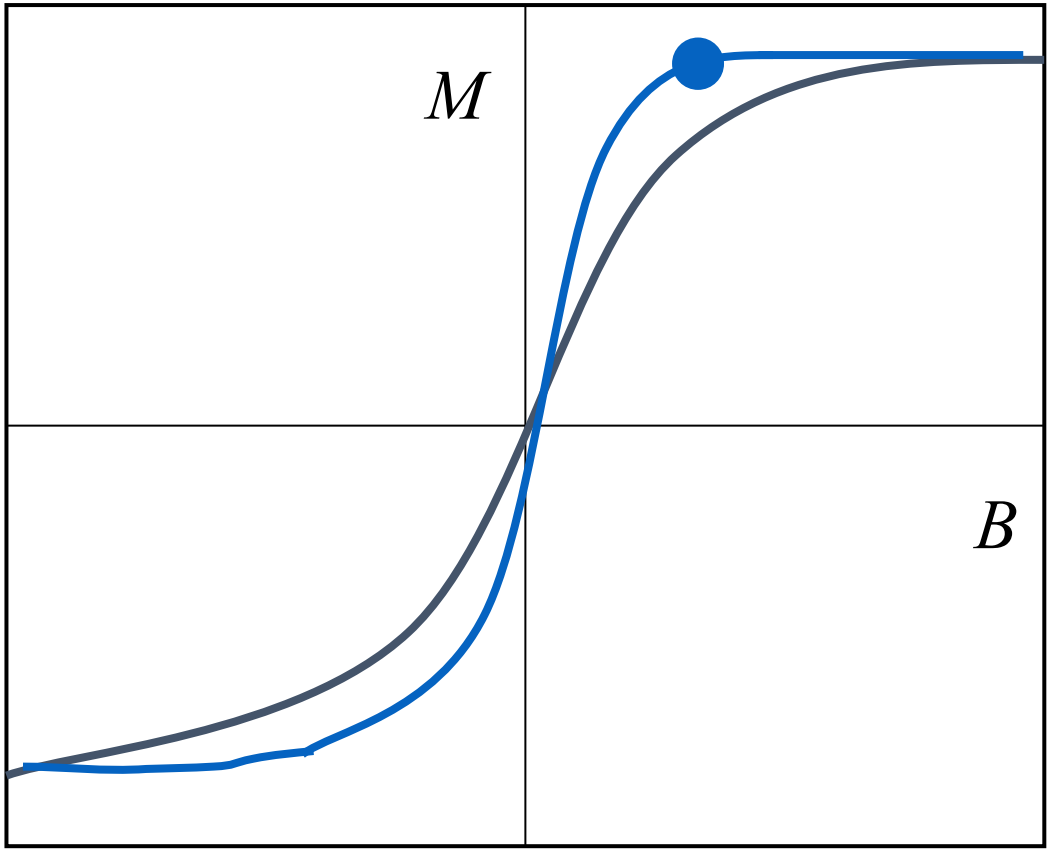

Superparamagnetism

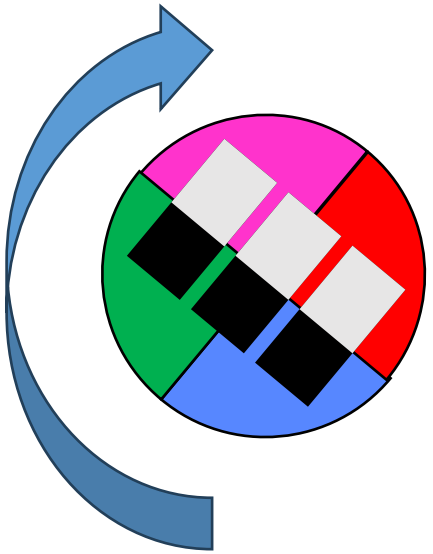

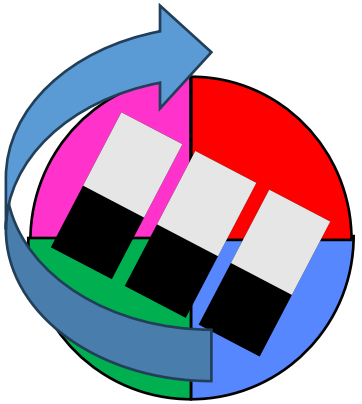

Brownian rotation vs. Néel rotation

(rotates whole NP)

(rotates just
the mag. moment)

MPI Principle

Superparamagnetic particle in a magnetic field

A response to the external field: alignment with

– Néel relaxation

– Brownian relaxation

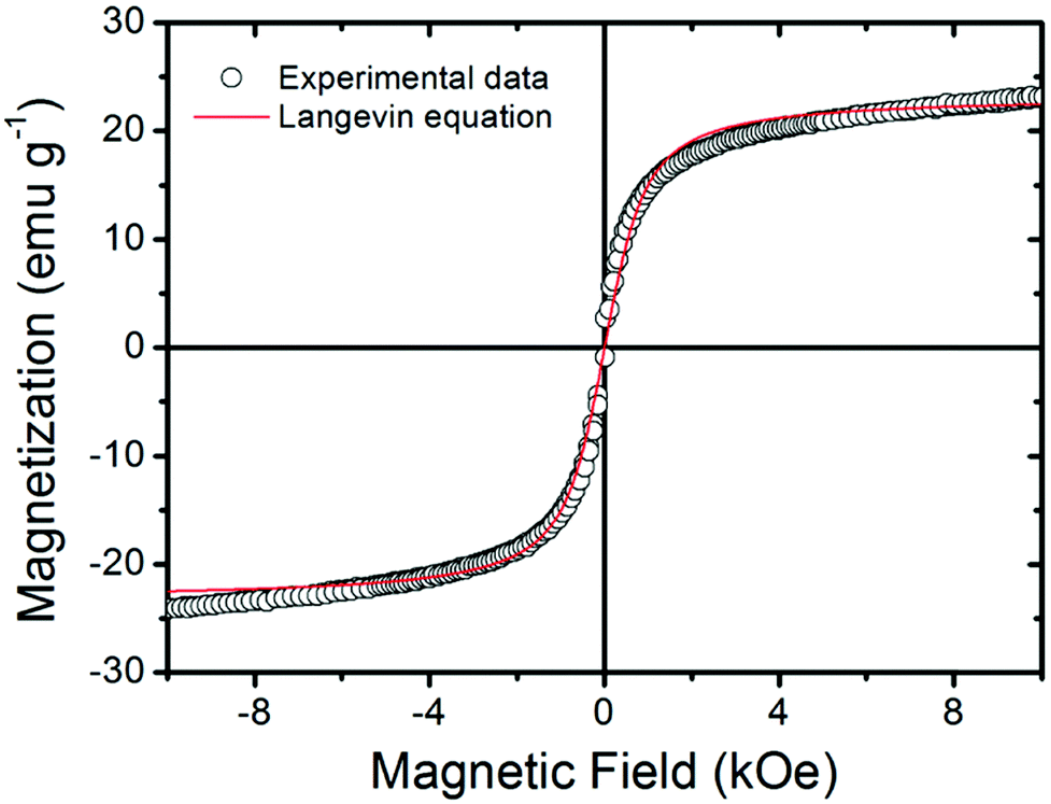

In equilibrium, magnetizaiton M of superparamagnetic particles (with a magnetic moment μ) in the external magnetic field B is described by Langevin equation

$$M(B) = N\,\mu\,\mathrm{L}(\mu B/kT)$$

Principle of MPI

External alternating mg. field („drive field“) induces change of magnetization

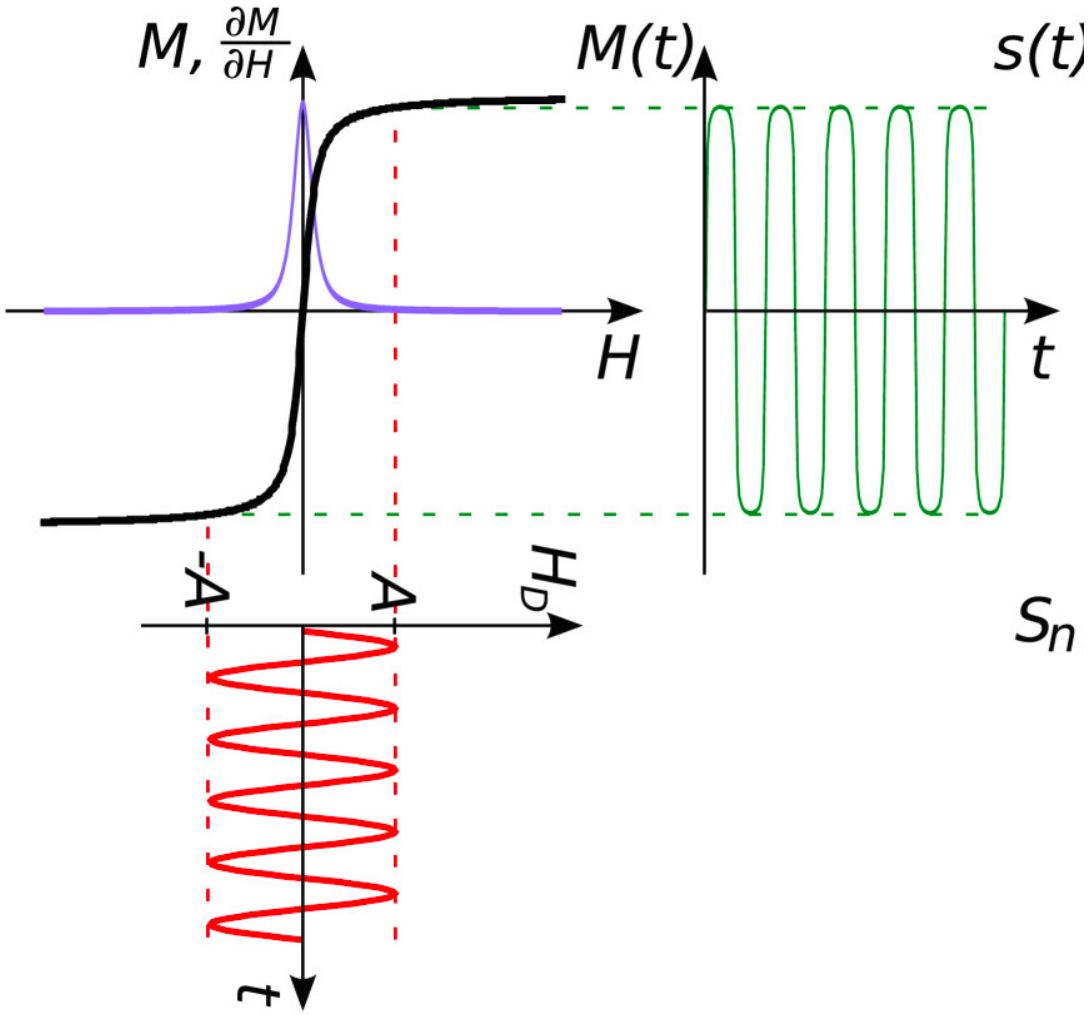

Principle of MPI

In the presence of a static external mg. field

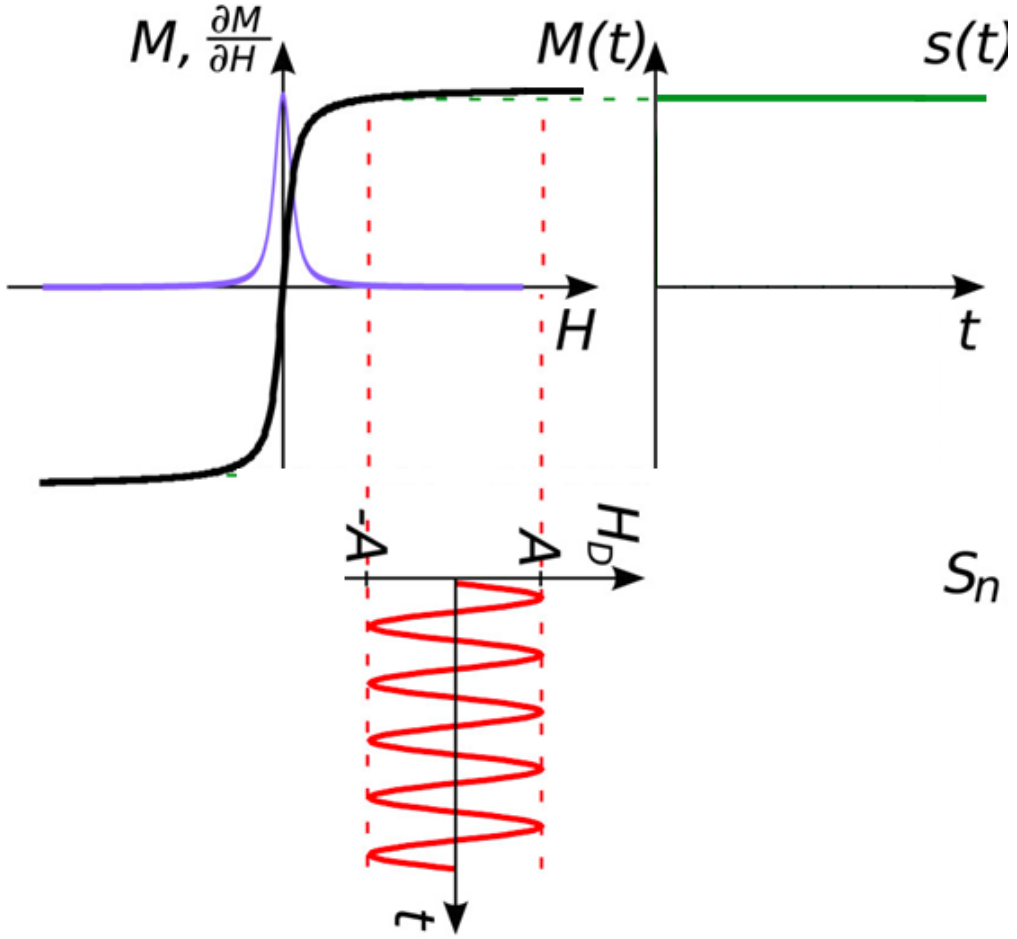

Nanoparticles are saturated, alternating field („drive field“) does not induce change of magnetization!

Principle of MPI

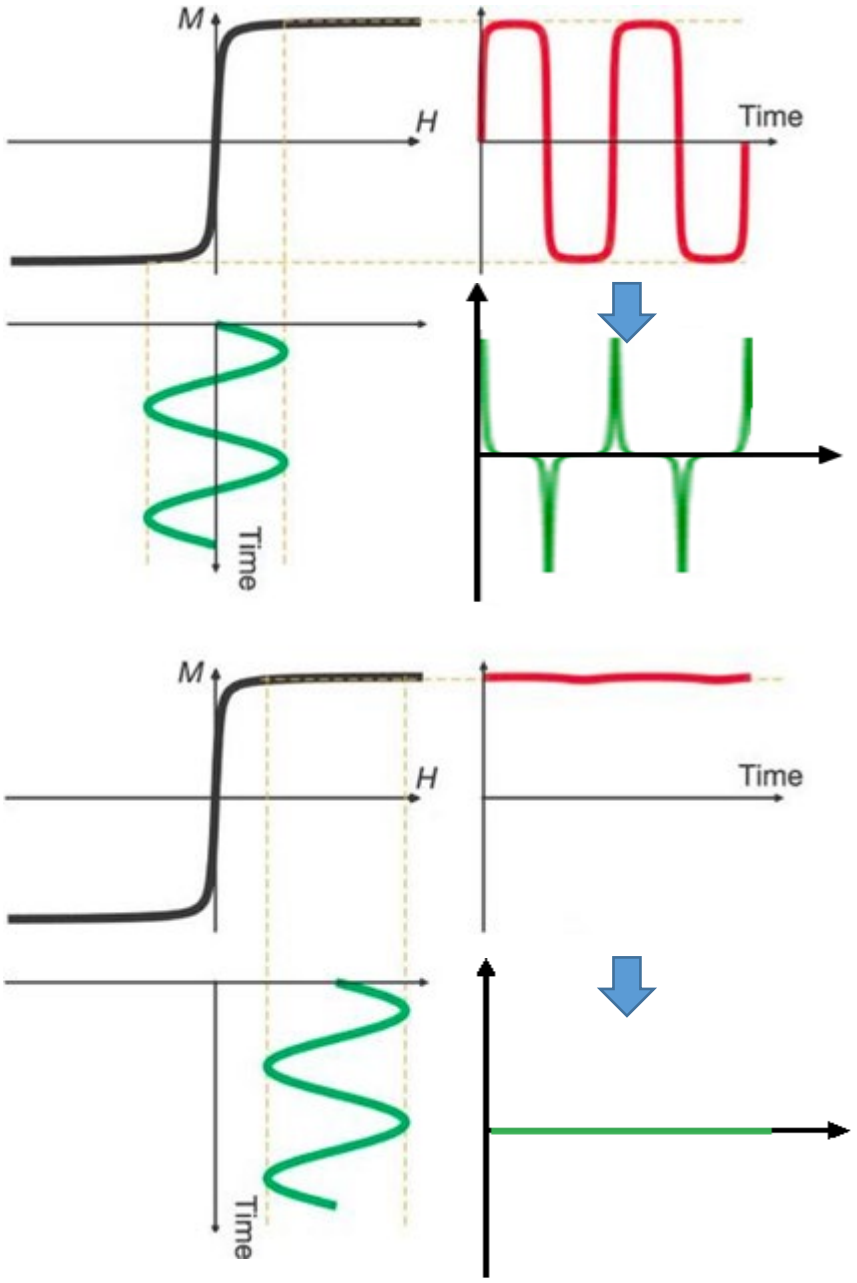

We do not detect magnetization, but its change = derivative!

At saturation, derivative is zero

Principle of MPI

External static gradient field in the space („selection field“)

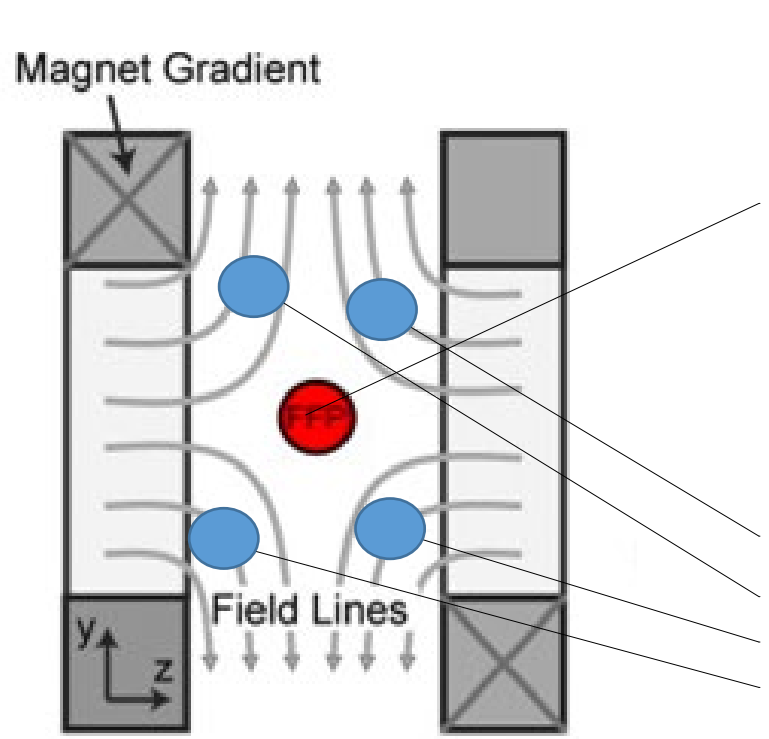

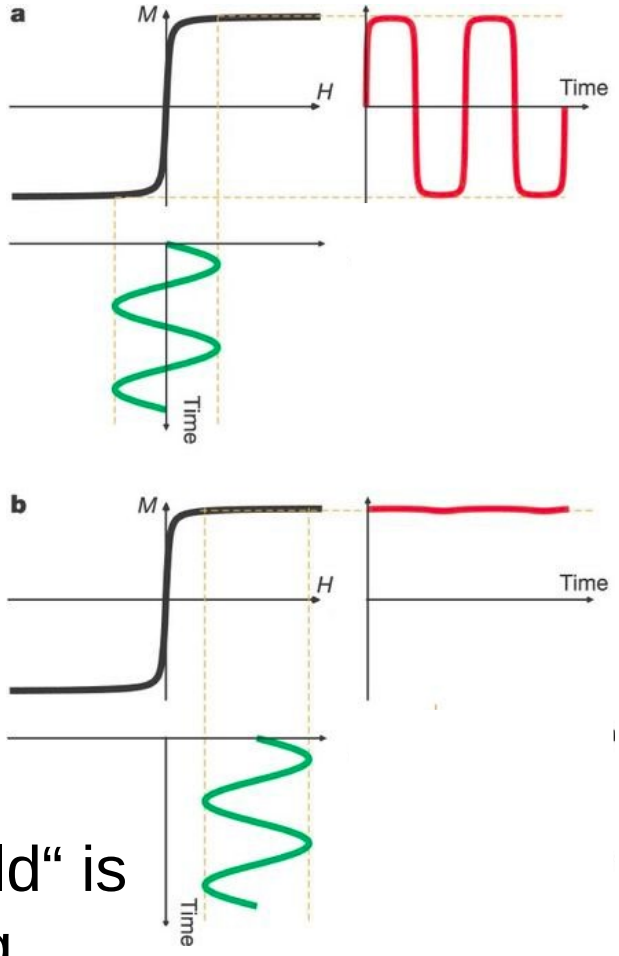

Change of magnetization induced by the „drive field“ is observed in a small region in the center, remaining particles are saturated

Principle of MPI

We can scan by the „field free point“ whole space and thus find out the nanoparticle distribution

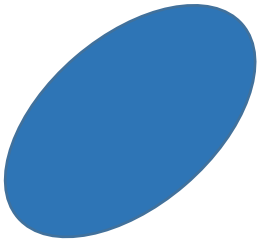

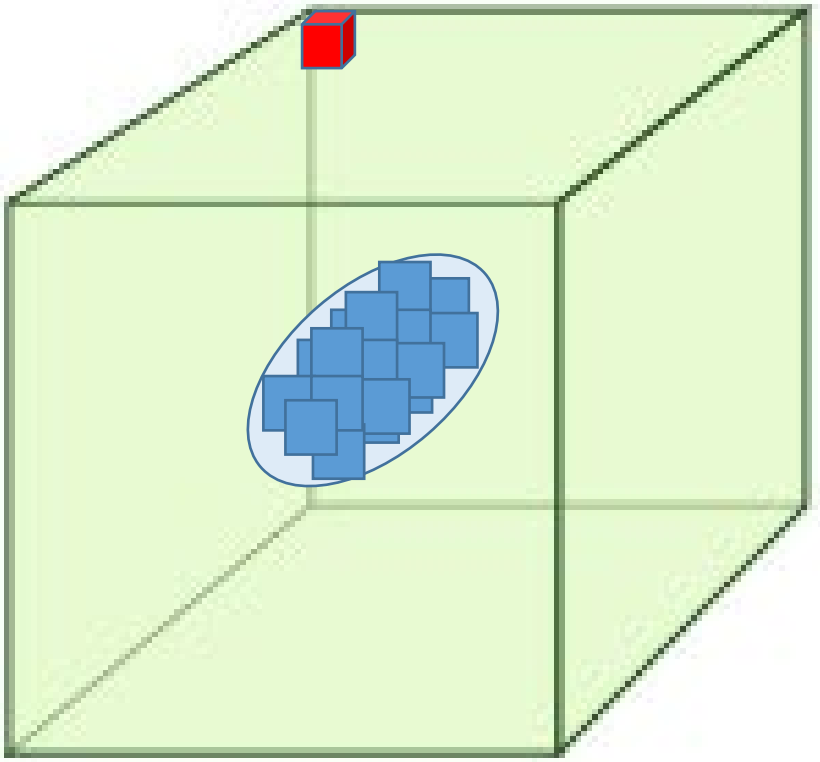

Problems

- Physical (acquisition during excitation)
- Technical (is it possible to build an apparatus with sufficient field strenghts?)
- Practical (sequential scanning of a 3D space would take ages)
- Material (pure superparamagnetic particles are needed, nontoxic, biocompatible…)

Acquisition during excitation

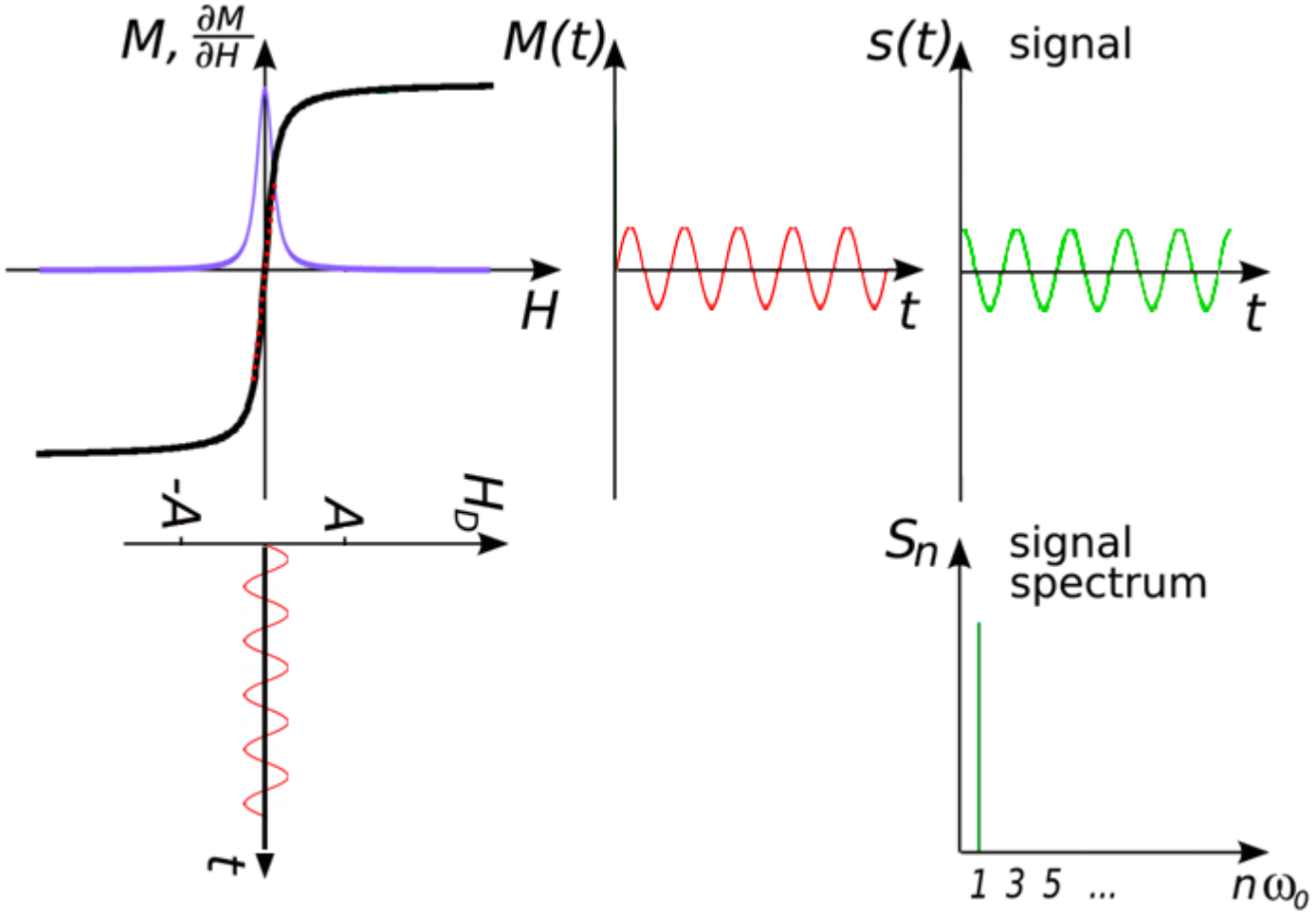

If amplitude of the alternating „drive field“ is low (i.e., in the linear part of the magnetization curve), the magnetization follows a sinus function and also the signal is sinusoidal

- We record one frequency only

Acquisition during excitation

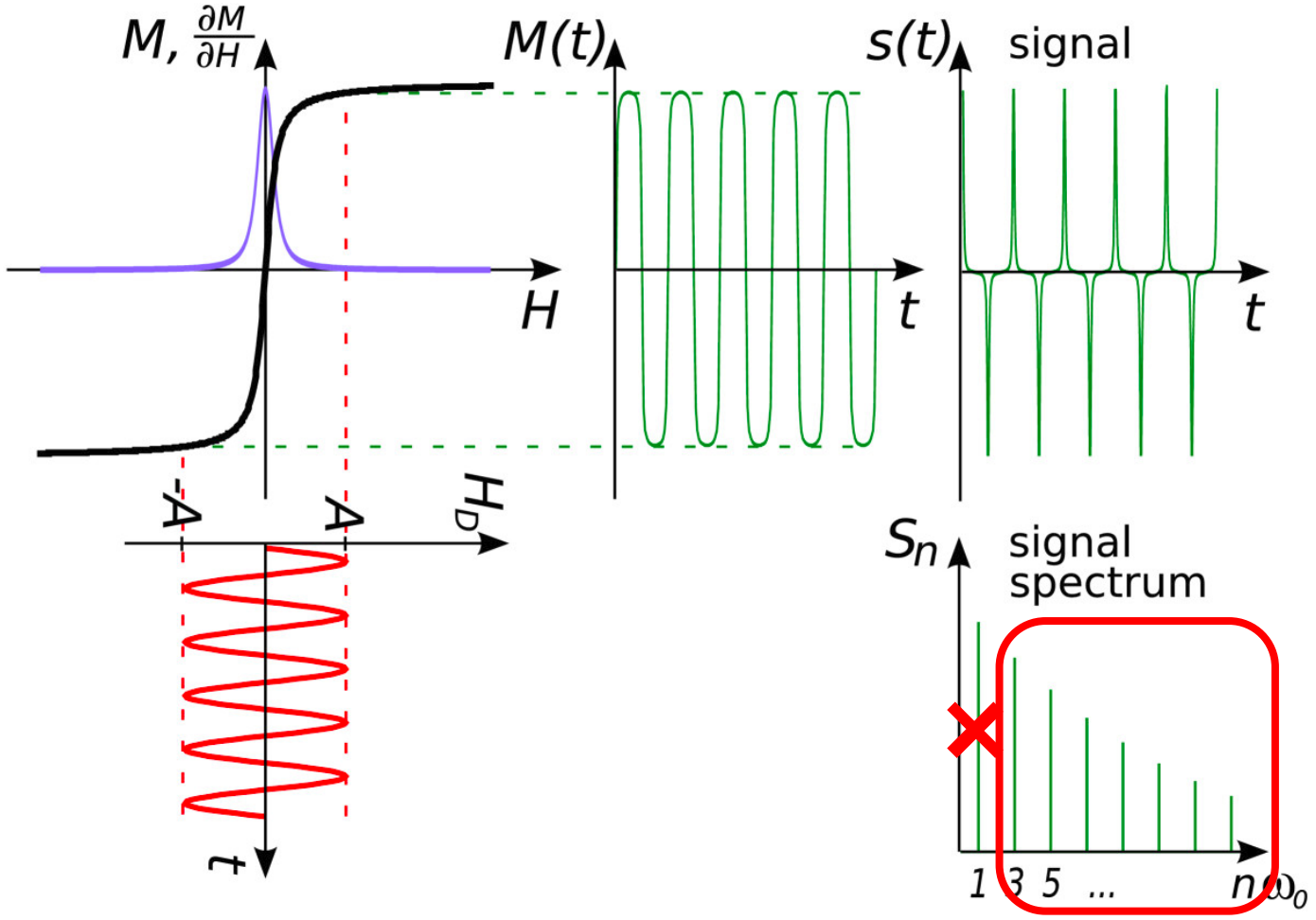

Amplitude of the alternating „drive field“ should reach non-linear part of the magnetizatin curve

- Then we record also higher harmonics; basic frequency can be filtered out

How to gain spatially resolved data?
Two approaches:

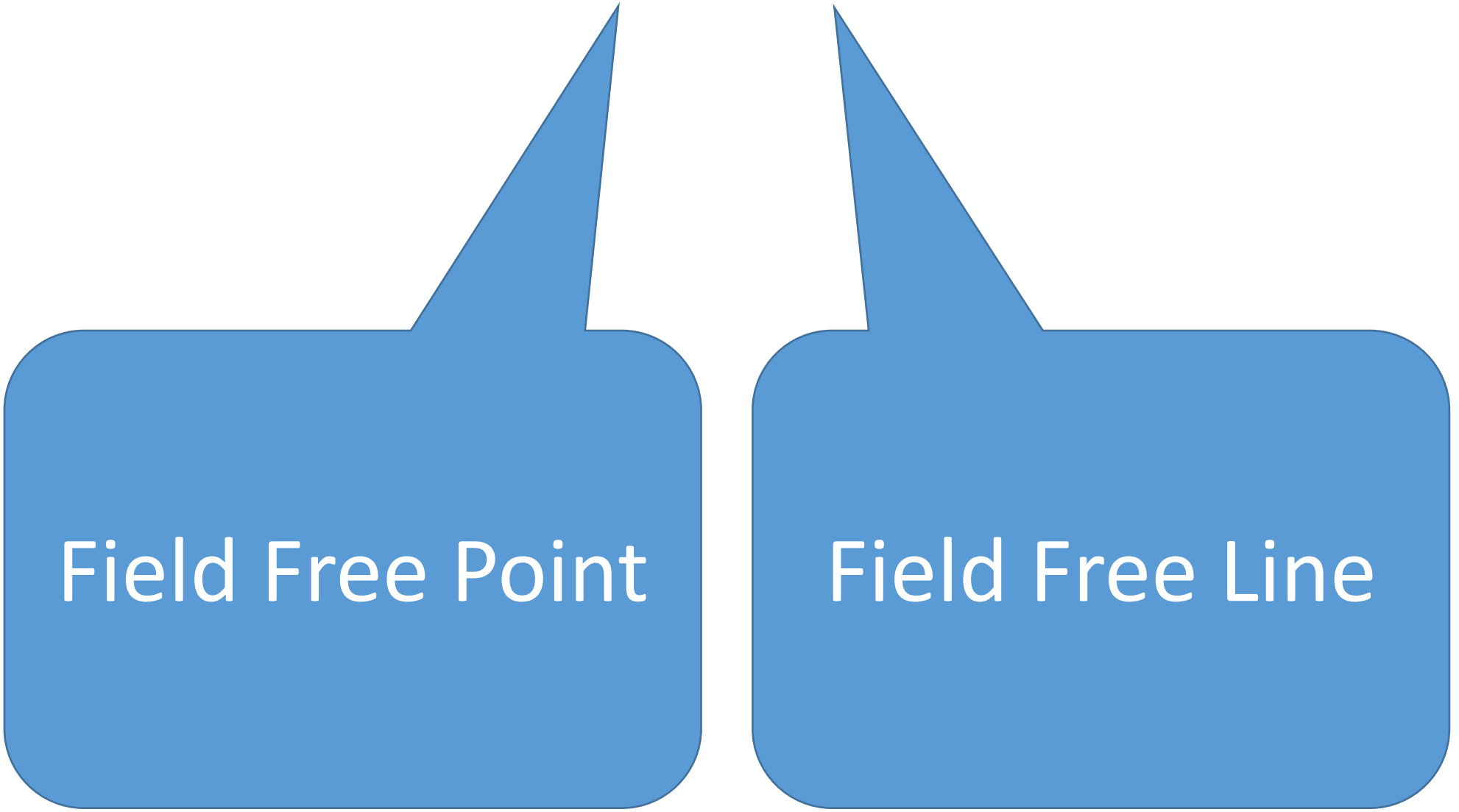

Field Free Point Approach

Alternating „drive field“ is applied in all three directions
Drive field simultaneously excites and moves the FFP

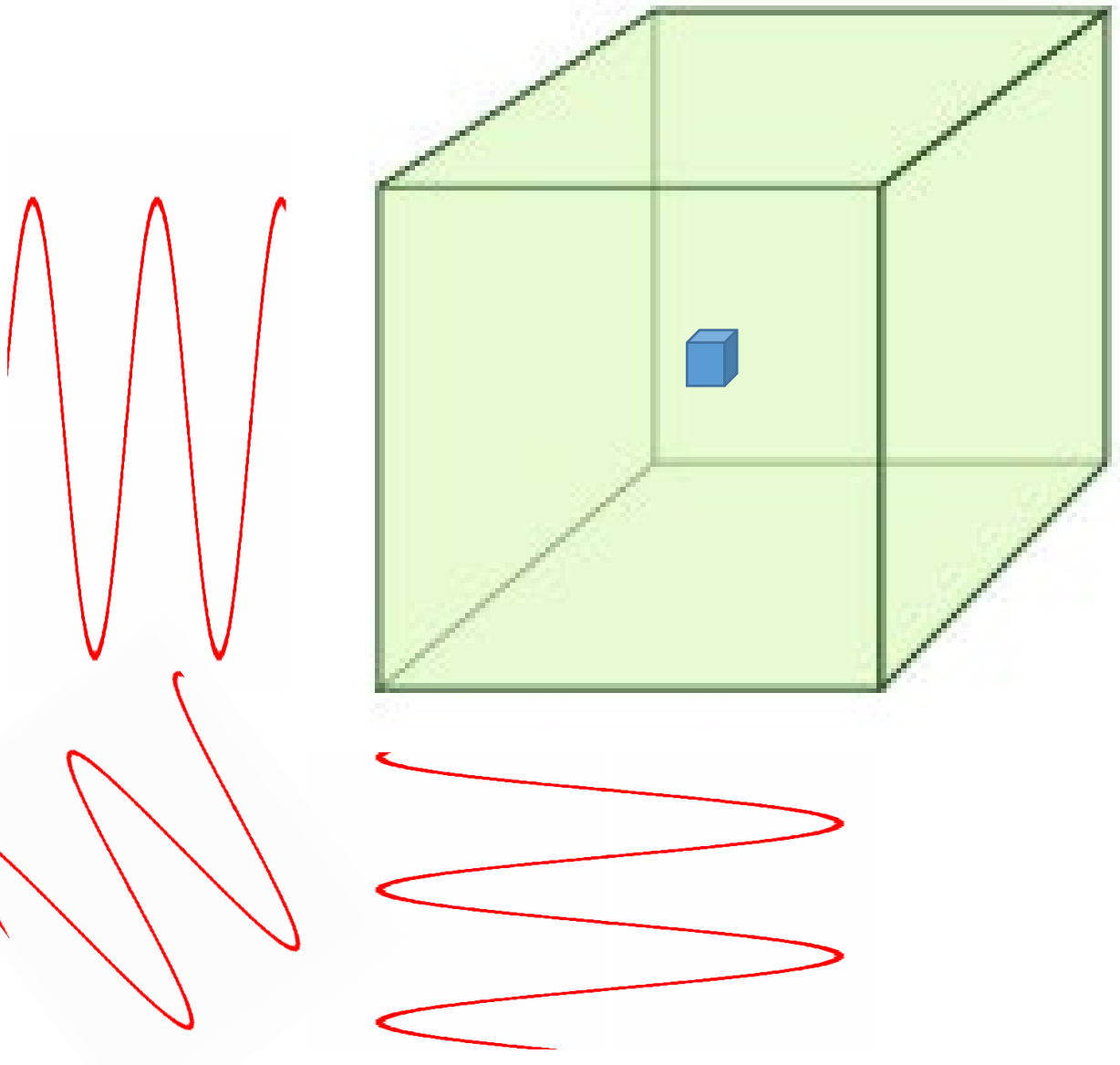

Field Free Point Approach

Alternating „drive field“ is applied in all three directions
Drive field simultaneously excites and moves the FFP

In one direction:

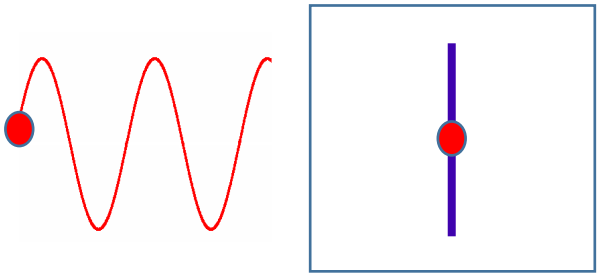

$x = 0, y = B \sin(b*t)$

2D Lissajous trajectory…

$x = A \sin(a*t+\delta), y = B \sin(b*t)$

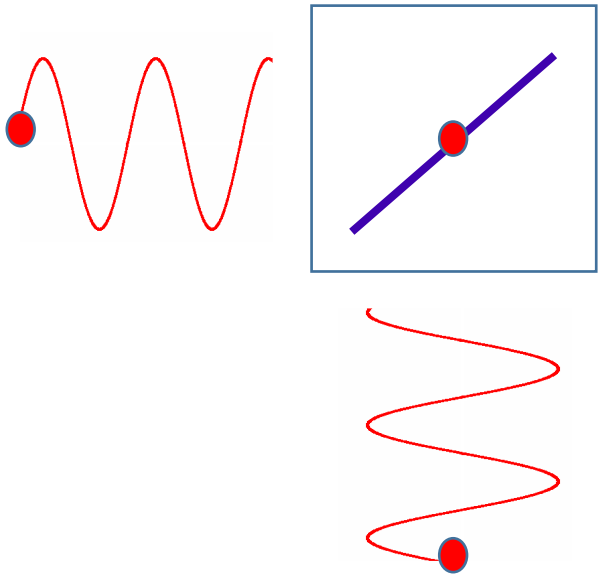

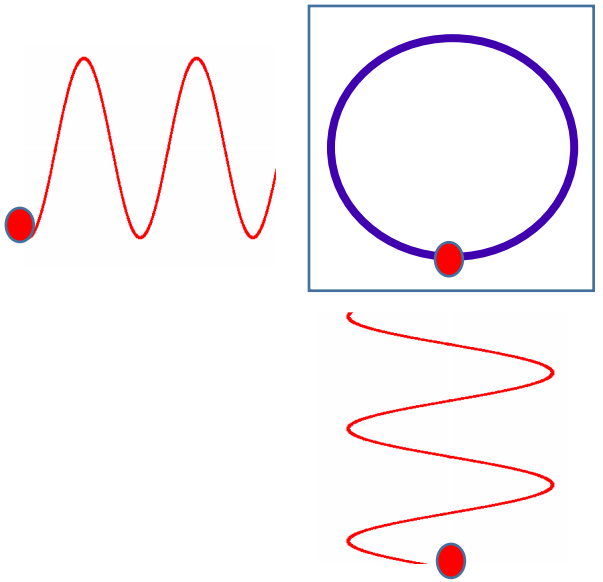

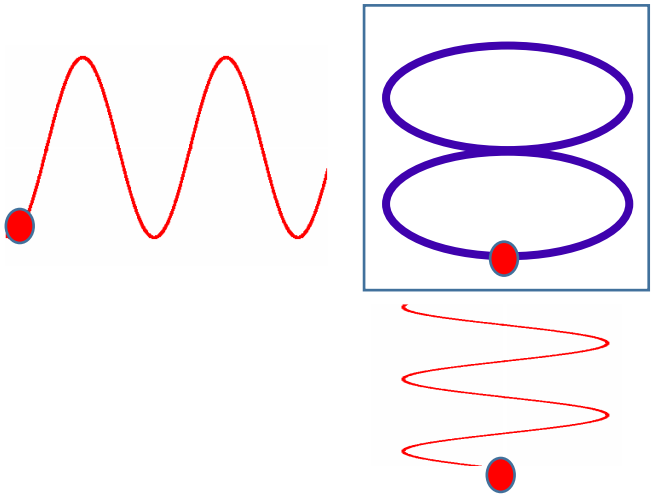

Field Free Point Approach

Alternating „drive field“ is applied in all three directions
Drive field simultaneously excites and moves the FFP

2D Lissajous trajectory… $x = A \sin(a*t+\delta)$, $y=B \sin(b*t)$

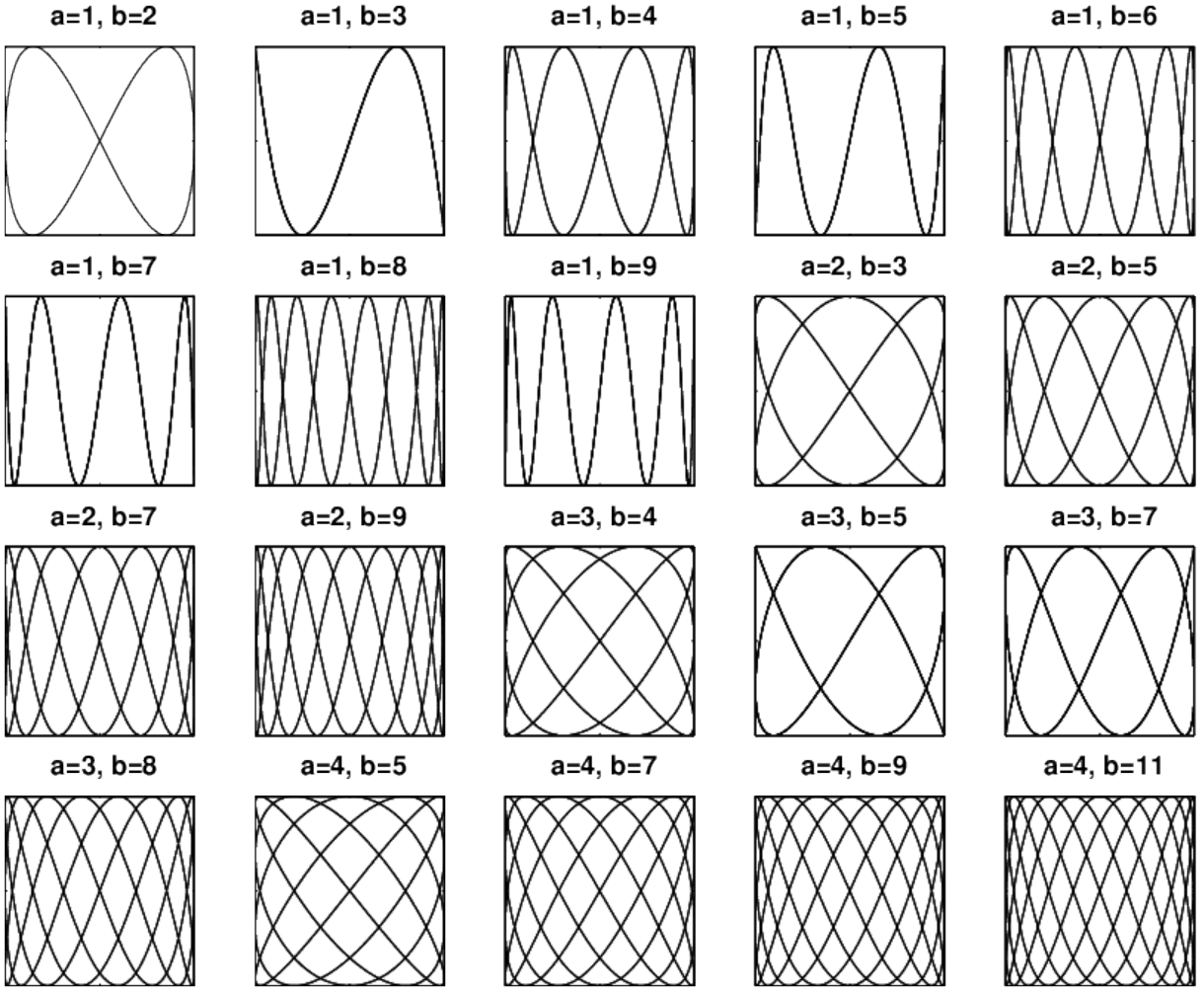

The higher the least common multiple of the frequencies, the more dense trajectory!

Field Free Point Approach

Alternating „drive field“ is applied in all three directions
Drive field simultaneously excites and moves the FFP

3D Lissajous trajectory… x = A sin(a*t+δ_1), y=B sin(b*t +δ_2), z=C sin(c*t)

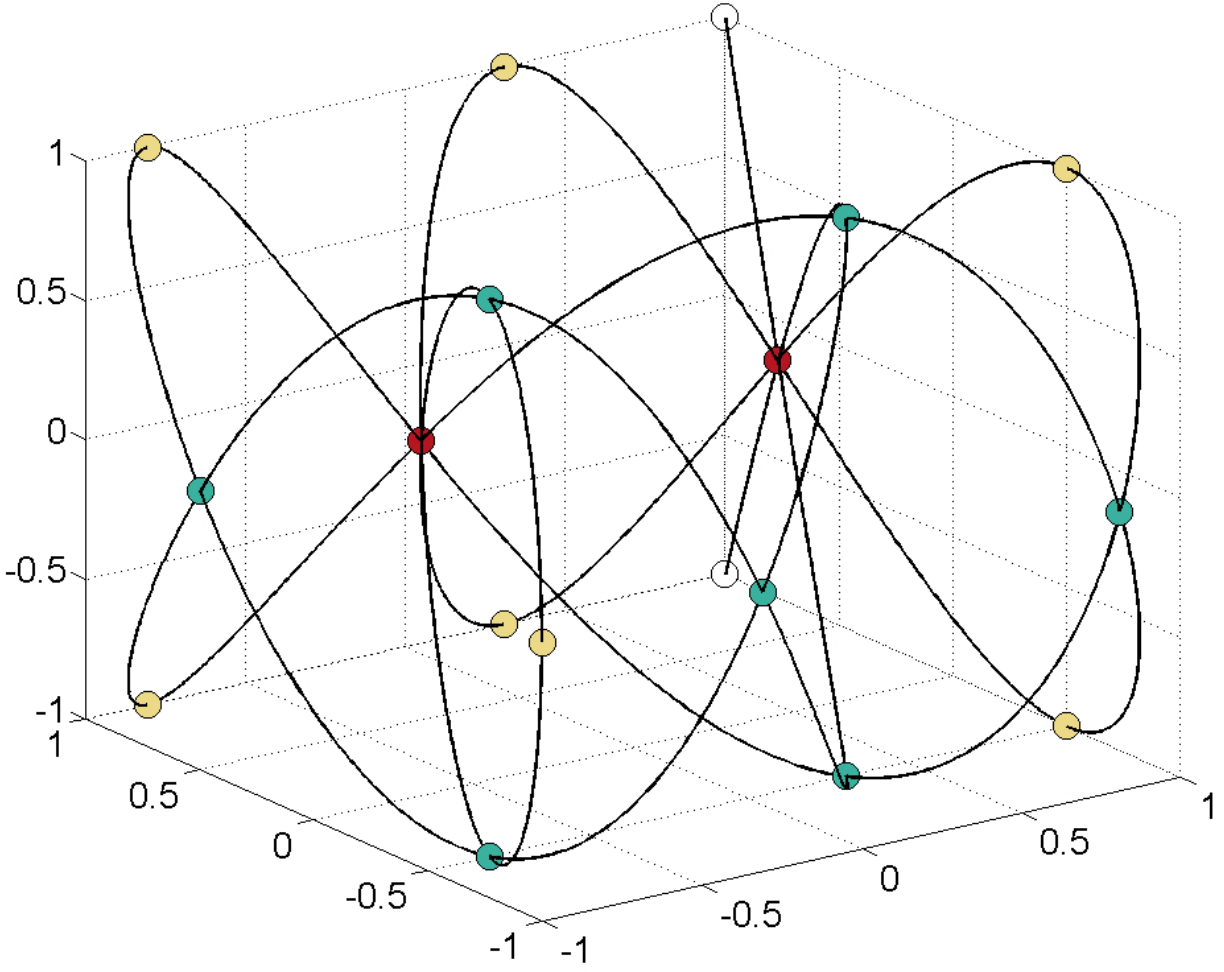

Virtual basic frequency f = 2.5 MHz,
Frequencies in three directions are derived as f/96, f/99, f/102

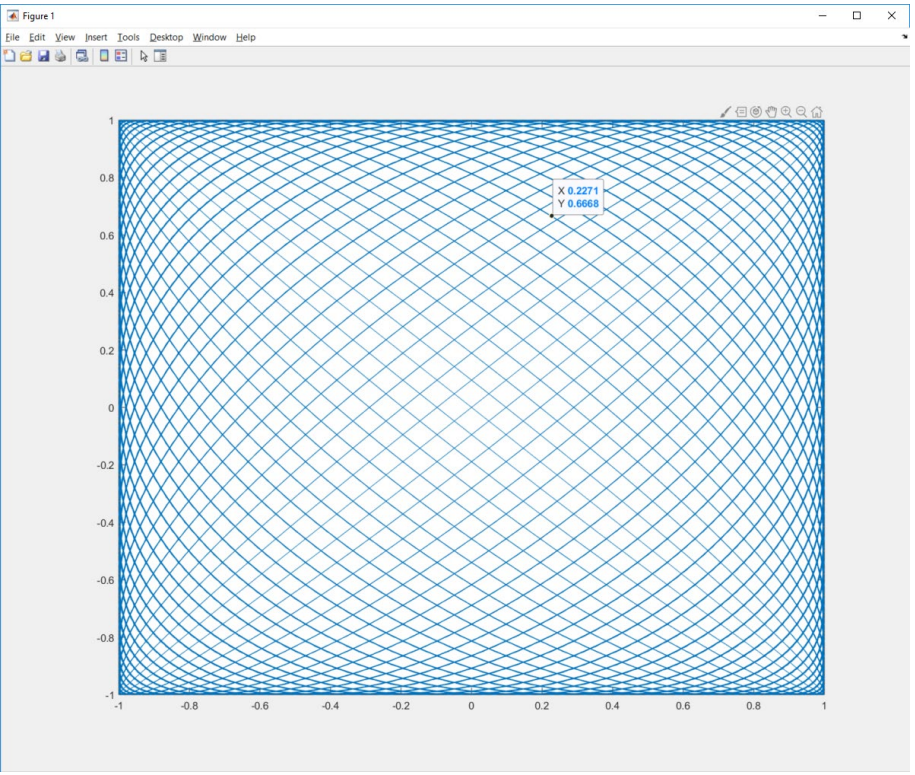

3D trajectory repeats with a frequency
2.5 MHz/53856 = 46,42 Hz (21.5 ms)

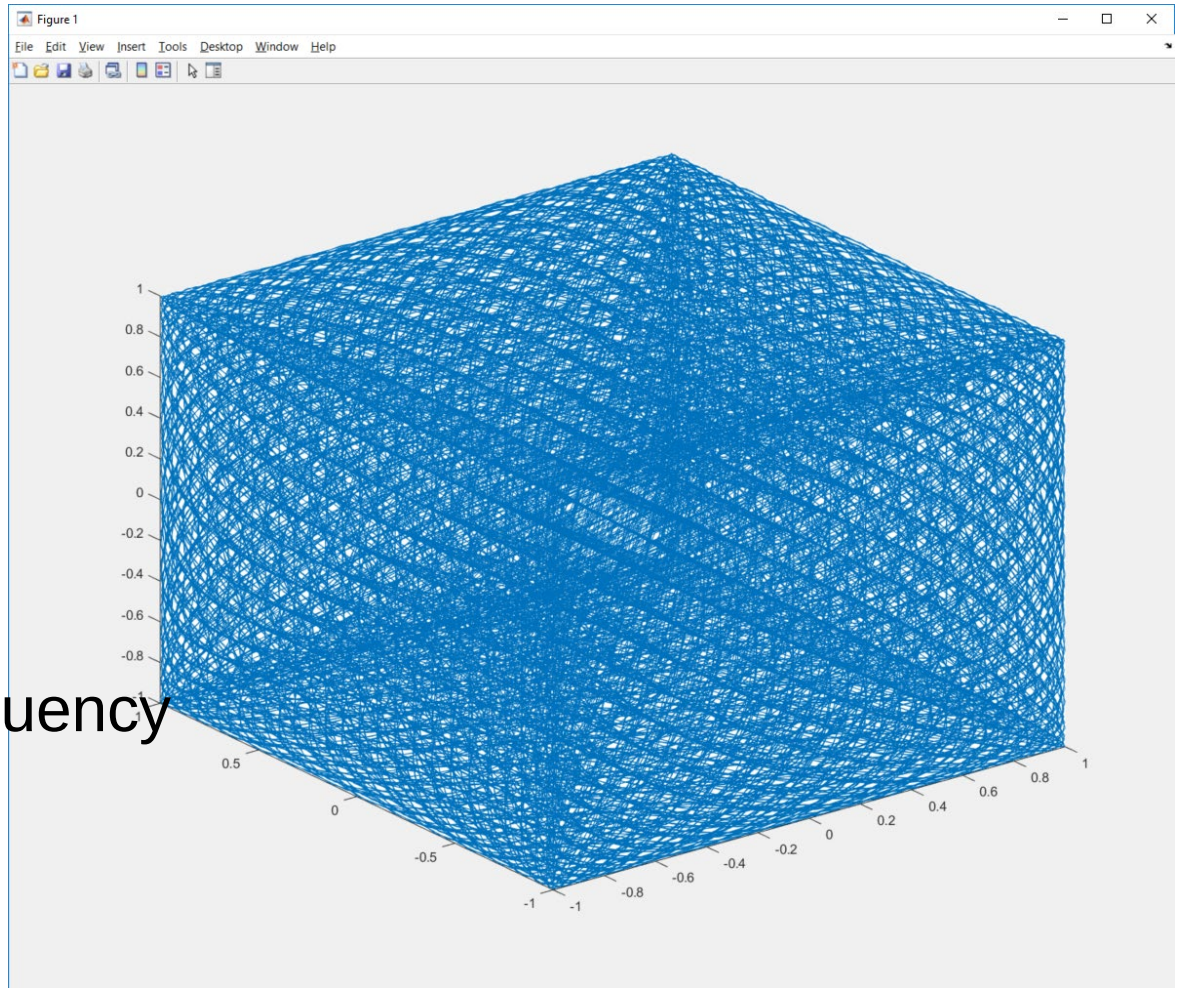

2D trajectory repeats with a frequency
2.5 MHz/3168 = 789.1 Hz
(1.27 ms)

How to decode the signal

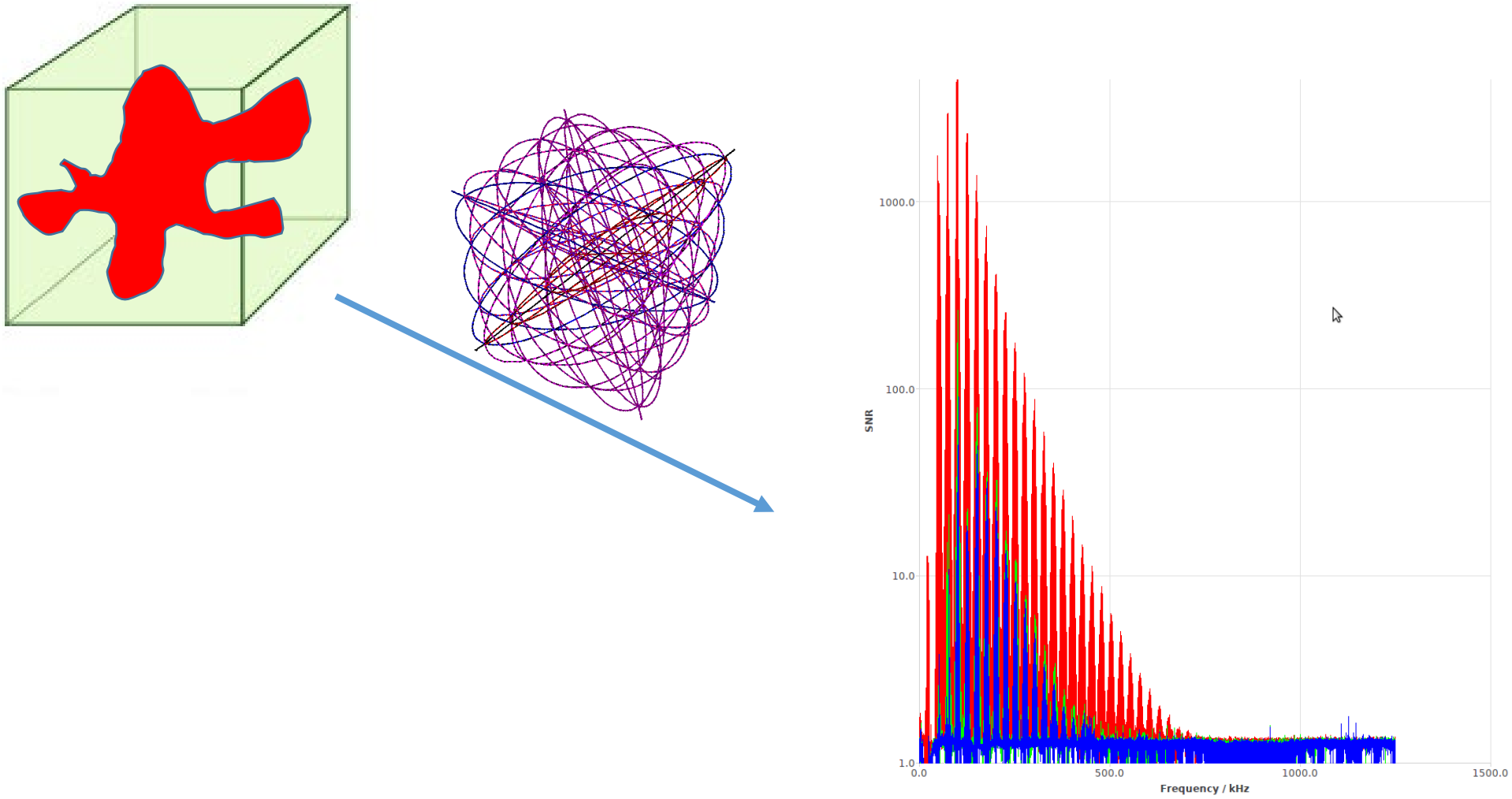

The acquired signal will be a sum of all the signals from the whole volume recorded along the Lissajous trajectory! **How to decode it**?

How to decode the signal

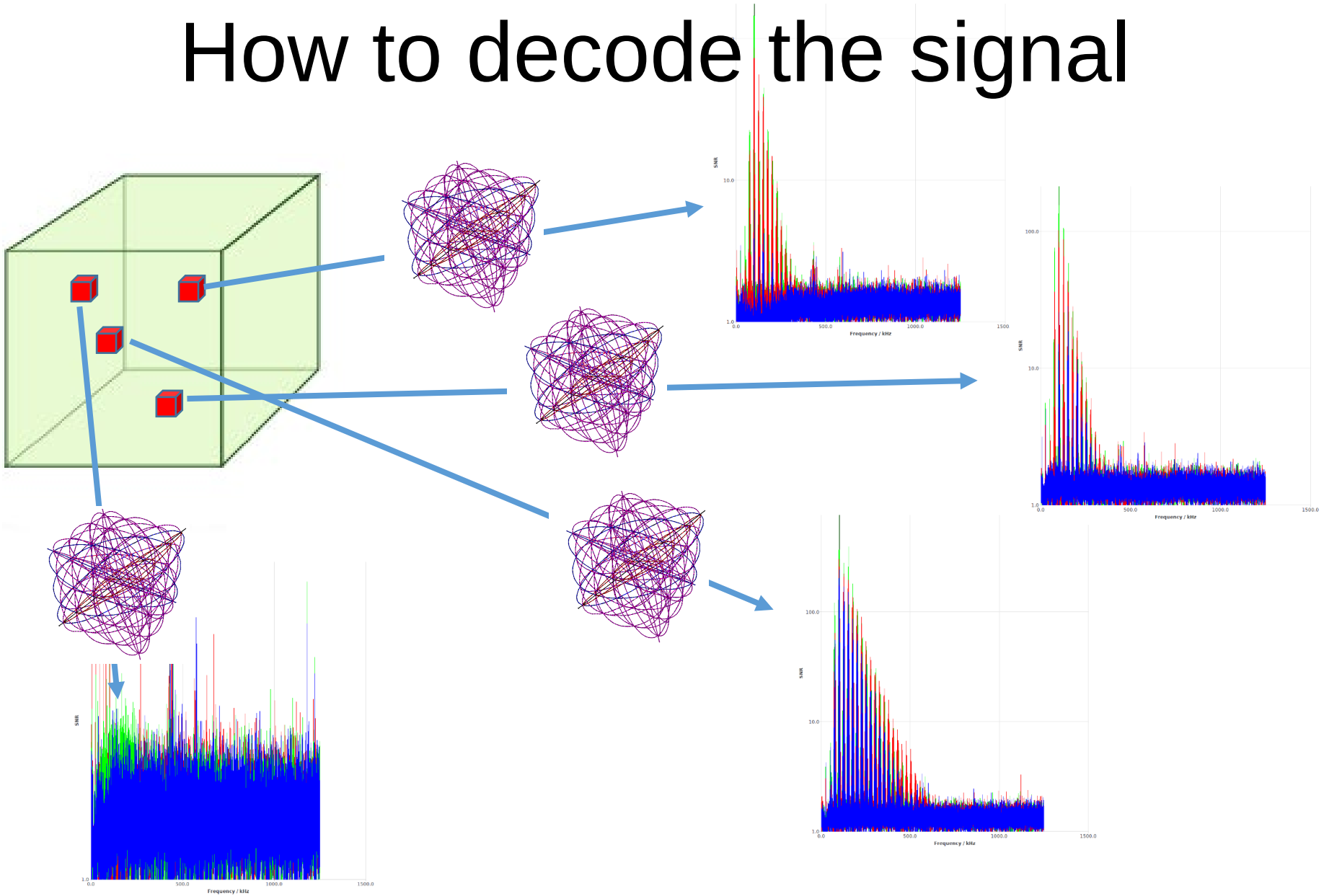

1. We perform a calibration using a known sample:
a step-by-step measurement in ALL points of the scanned space –
and its signal is recorded along the Lissajous trajectory

How to decode the signal

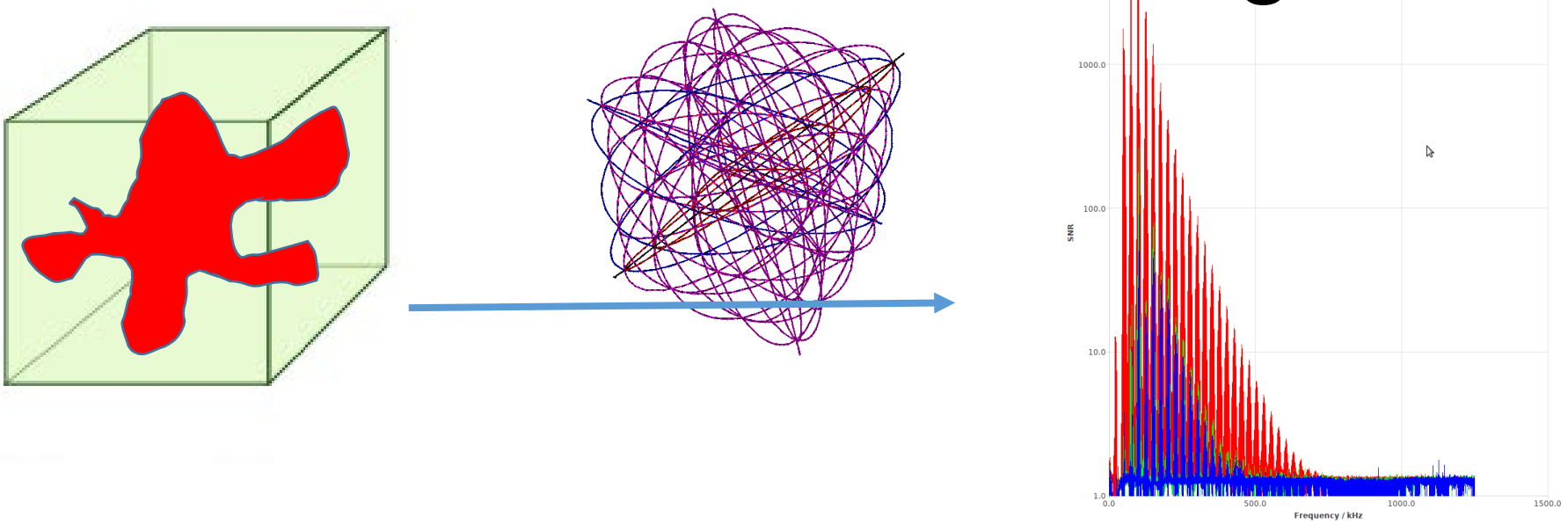

2. Unknown sample is scanned once, its signal contains information from the whole volume.

How to decode the signal

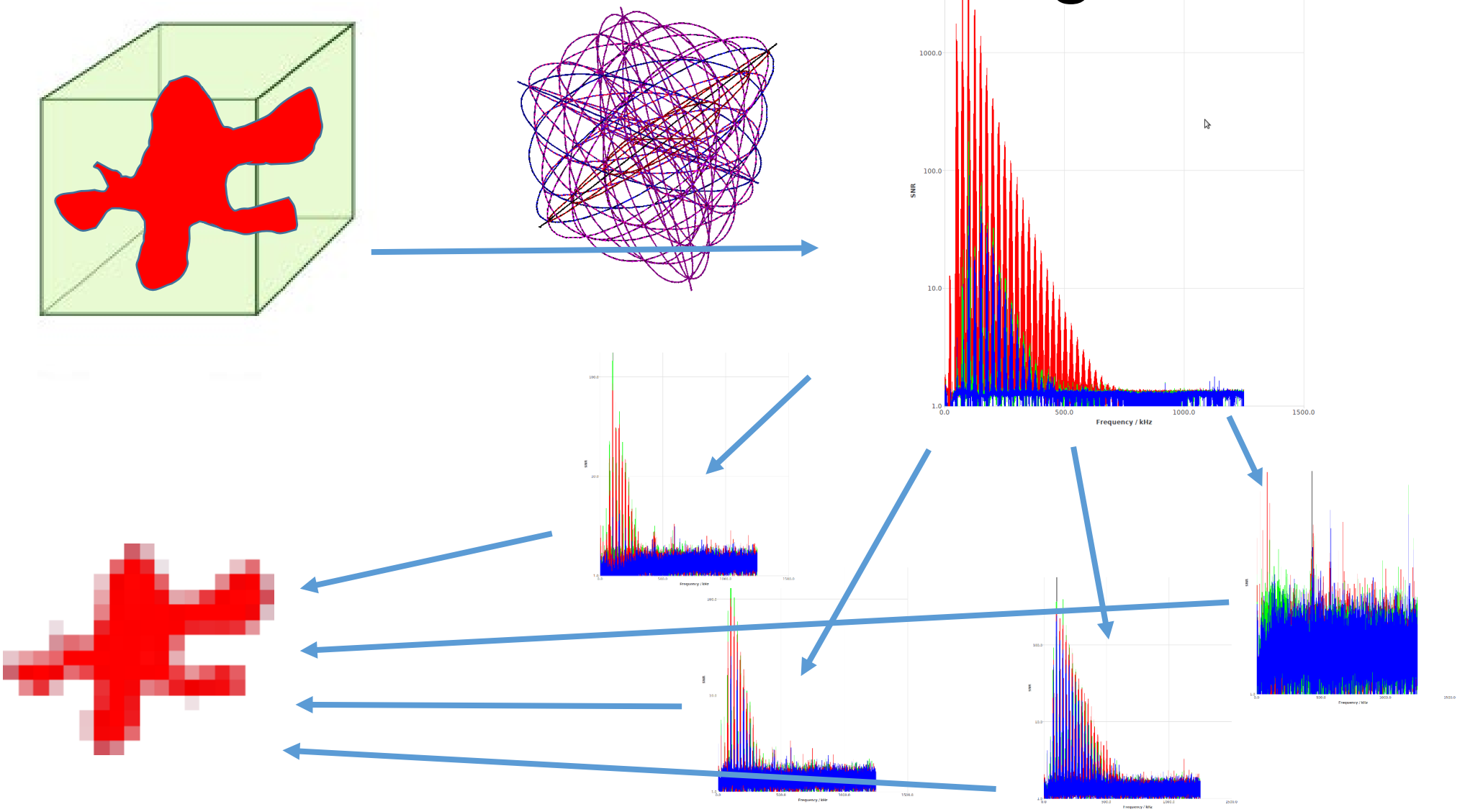

3. Signal of the sample is fitted by a linear combination of calibration signals, the linear coeficients define distribution of the nanoparticles. The sample has to contain the SAME particles!

Is it possible to decode the signal directly?

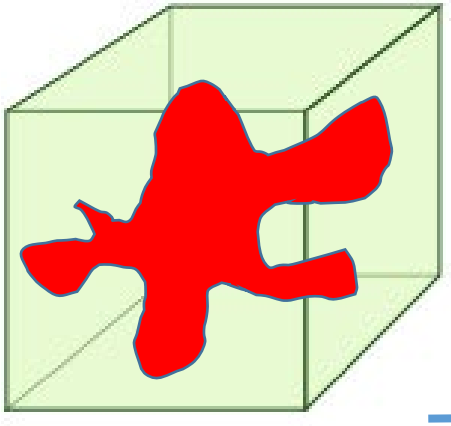

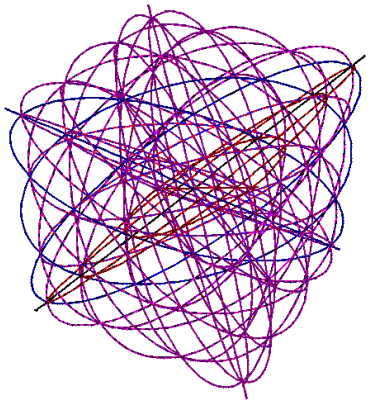

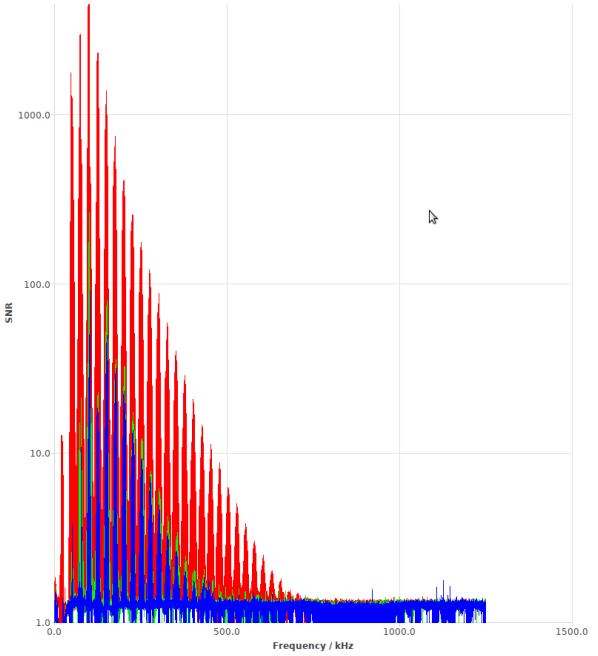

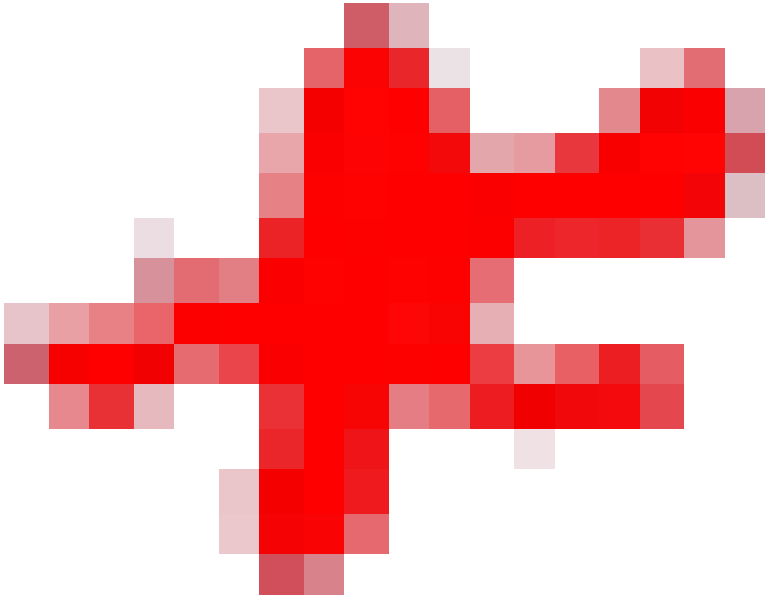

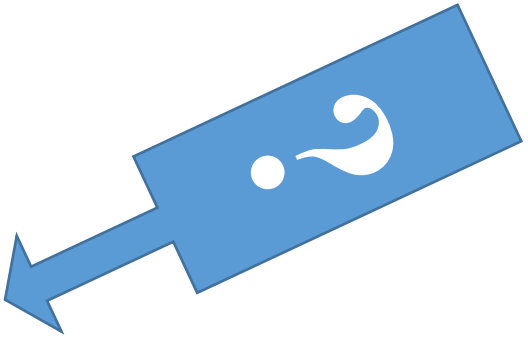

Probably not unambiguously…

Field Free Line Approach

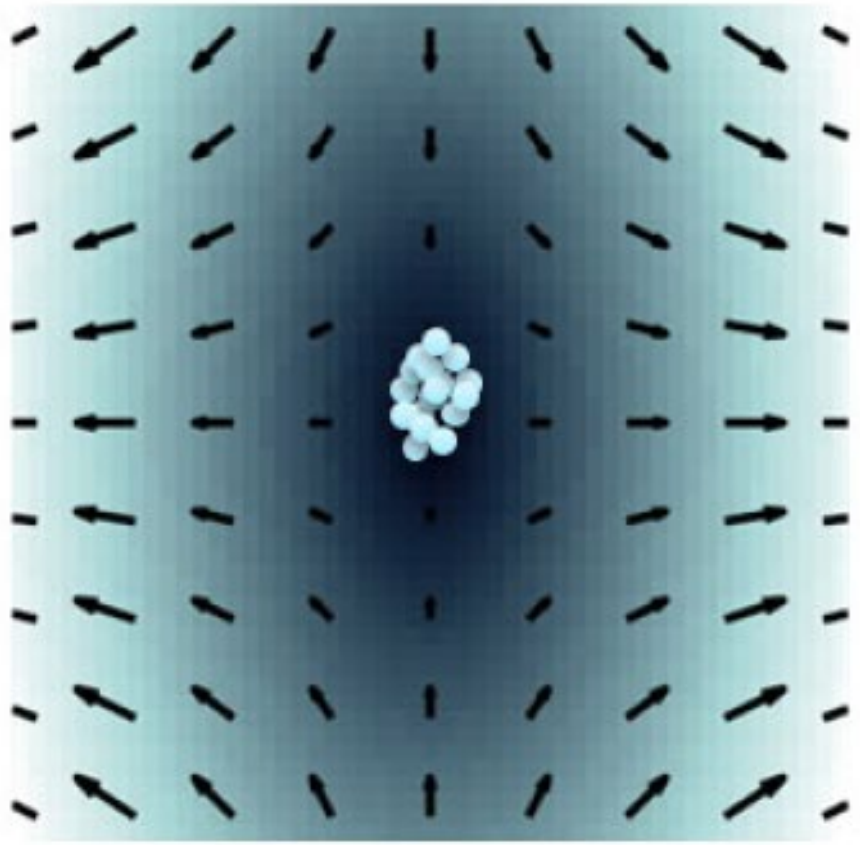

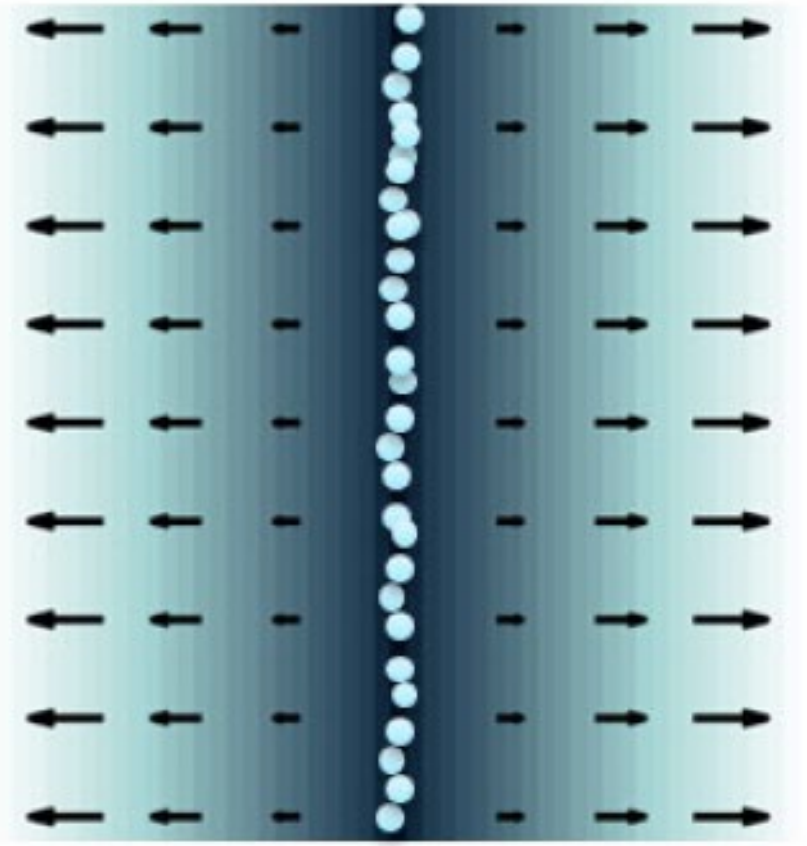

Field Free Line Approach

Signal distribution in x-y plane:

$$f(\mathbf{x}) = f(x,y)$$

Signal along a straight line *L*:

$$Rf(L) = \int_L f(\mathbf{x})\,|d\mathbf{x}|$$

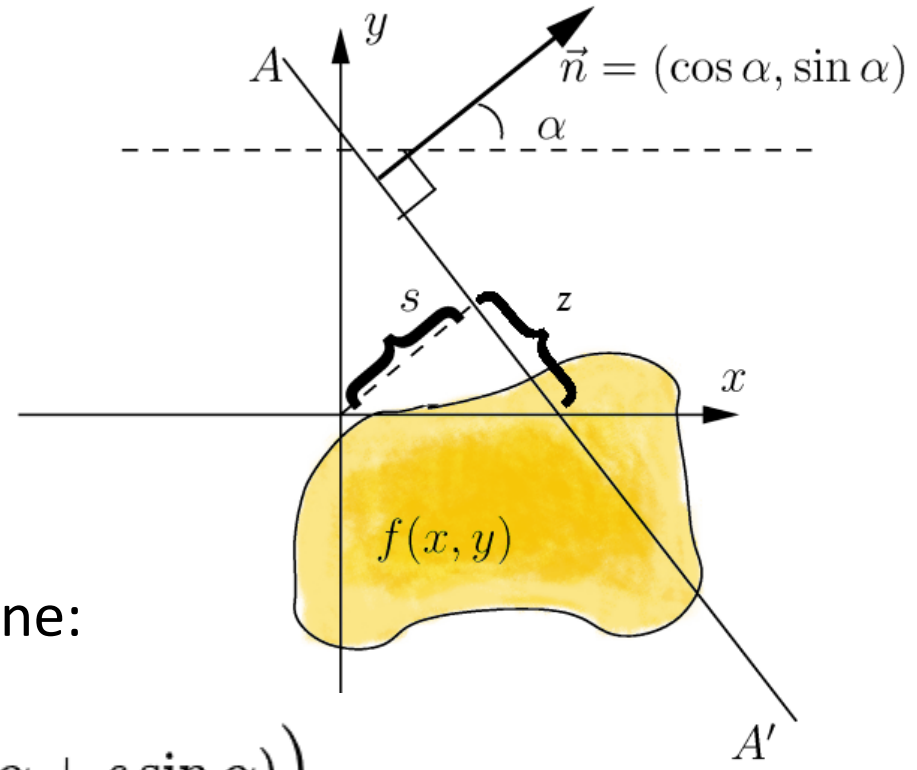

Introducing a parametric equation of a line:

$$(x(z), y(z)) = \Big((z\sin\alpha + s\cos\alpha), (-z\cos\alpha + s\sin\alpha)\Big)$$

Then:

$$Rf(\alpha, s) = \int_{-\infty}^{\infty} f(x(z), y(z))\,dz = \int_{-\infty}^{\infty} f\Big((z\sin\alpha + s\cos\alpha), (-z\cos\alpha + s\sin\alpha)\Big)\,dz$$

(Ray integral – Radon transformation)

Field Free Line Approach

Inverse Radon transformation – back-projection:

Search for

$$f(\mathbf{x}) = f(x,y)$$

in $$Rf(\alpha, s) = \int_{-\infty}^{\infty} f(x(z), y(z))\, dz$$

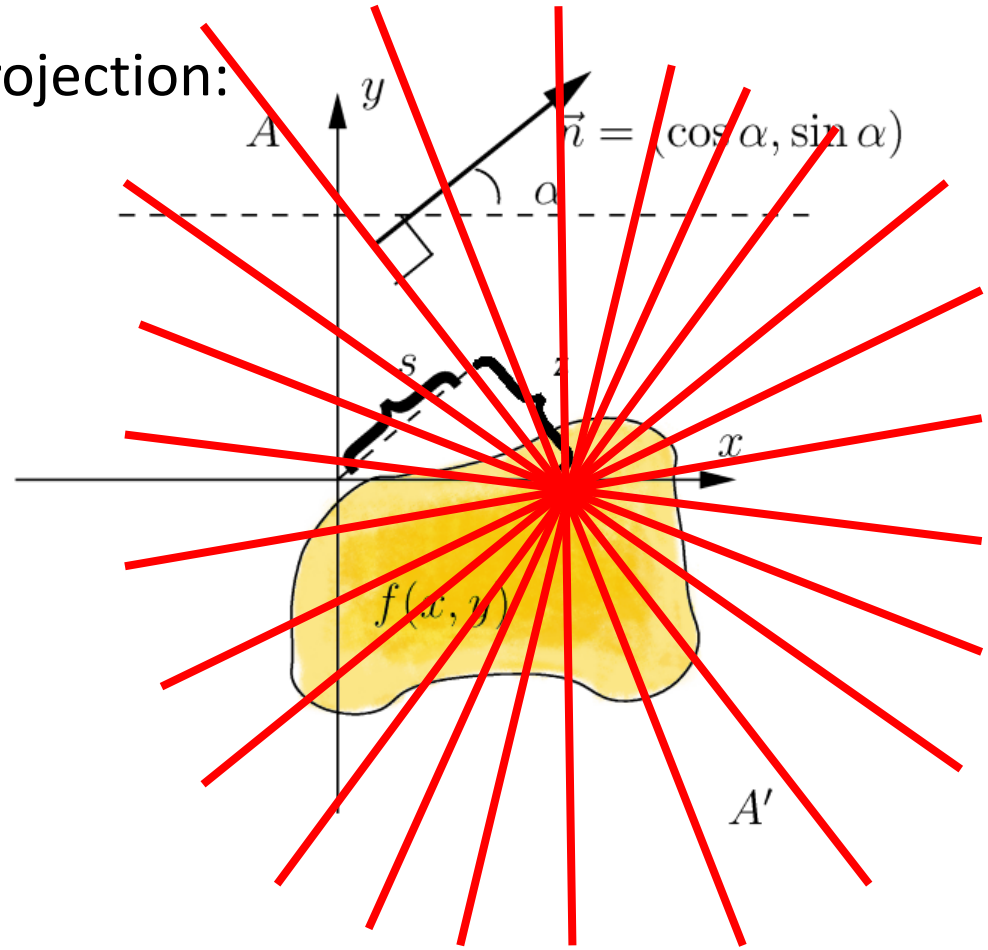

→ → necessary to fill Radon space by measurement at various angles α

As there is a limited number of α (discrete values), a discrete inverse Radon transformation is needed

Field Free Line Approach

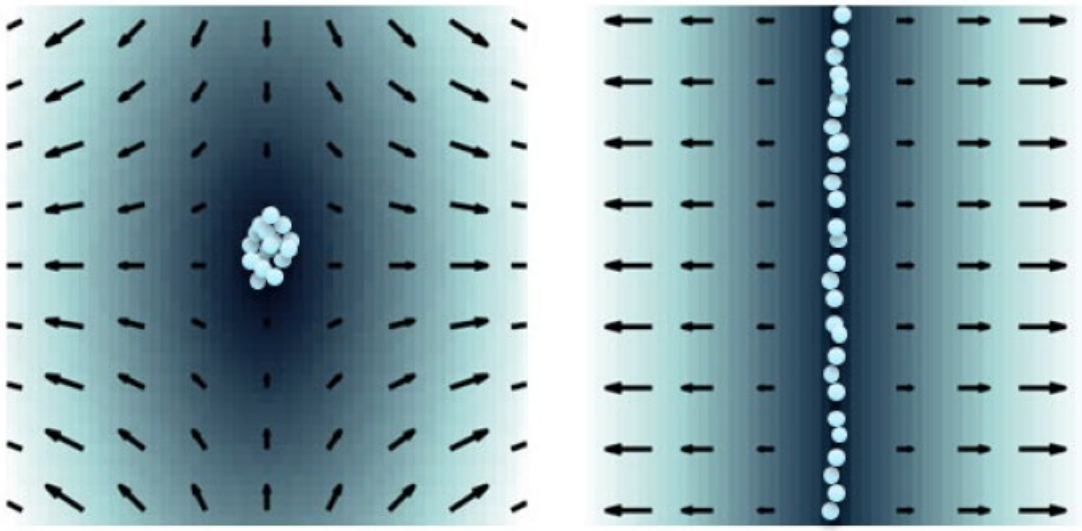

Advantages

- Higher sensitivity (obtaining higher signal during a single scan)
- Easier reconstruction using Radon transformation

Scanning volume in FFP method

Gradient „selection field“ and alternating „drive field“ define the scanning volume

14 mT + 2.5 T/m: 32 × 32 × 16 mm^3

To cover a volume of a mouse: 48 × 36 × 24 mm^3 (DF 14 mT; 9 mT; 14 mT, SF = 1 T/m)

Lower gradients increase the volume, but decrease spatial resolution!

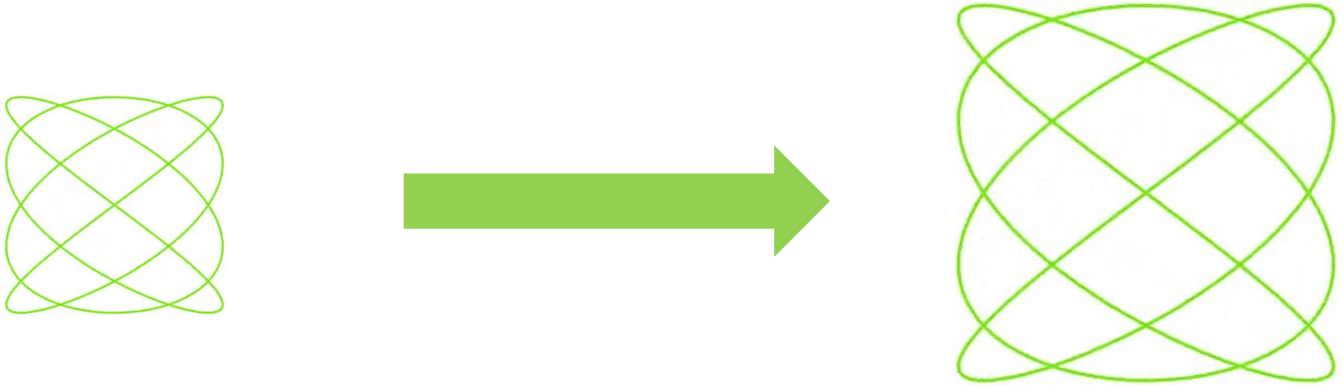

Low gradients stretch the same field range into bigger volume, but the data have same size

Scanning volume

FOV can be enlarged

- „table move“ – shift of the scanned sample, a sequence of images
- is then merged into one
- focus fields – another magnetic fields, which shifts FOV in the space

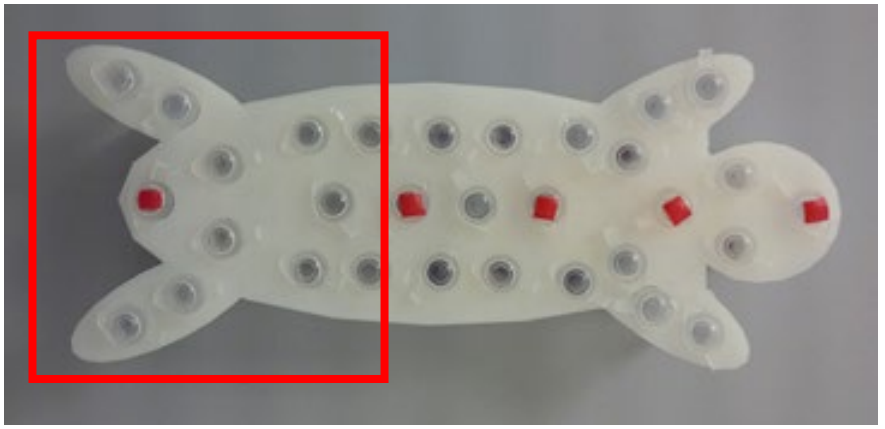

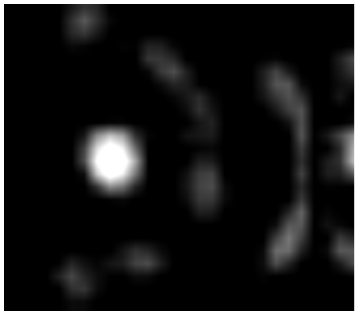

Scanning volume

FOV can be enlarged

- „table move“ – shift of the scanned sample, a sequence of images is then merged into one
- focus fields – another magnetic fields, which shift FOV in the space

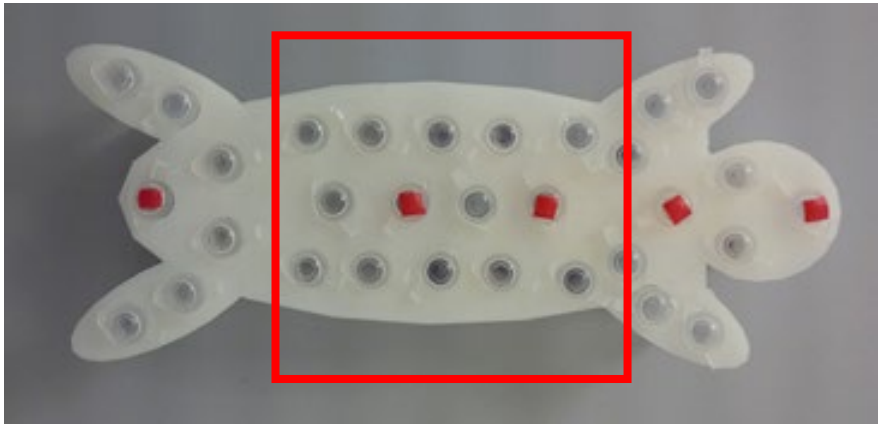

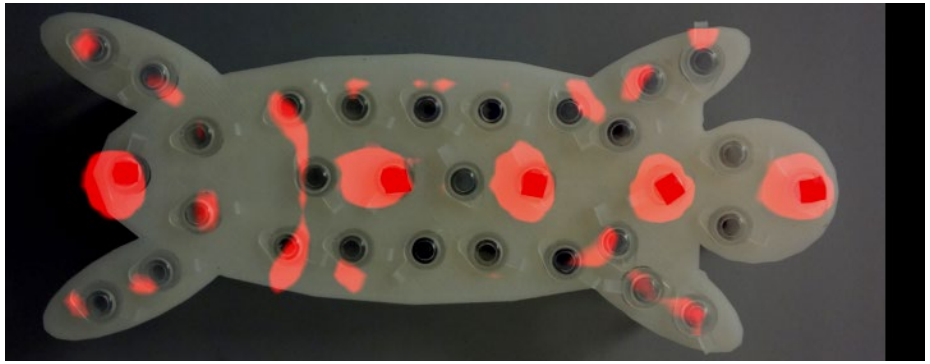

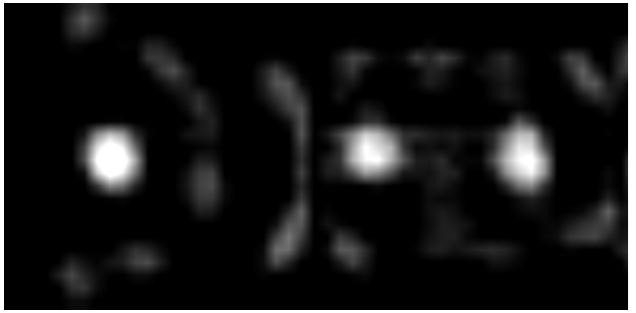

Scanning volume

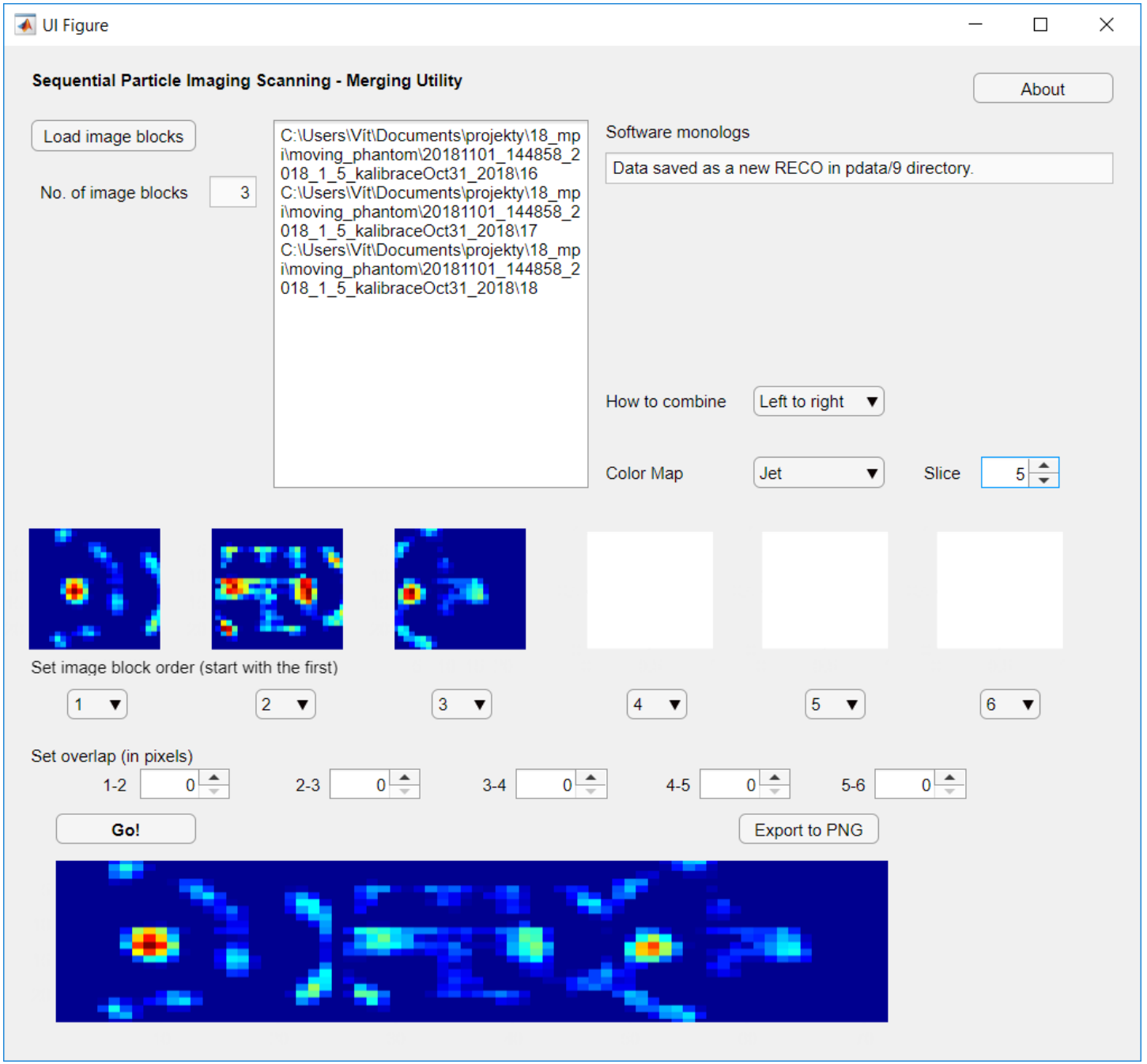

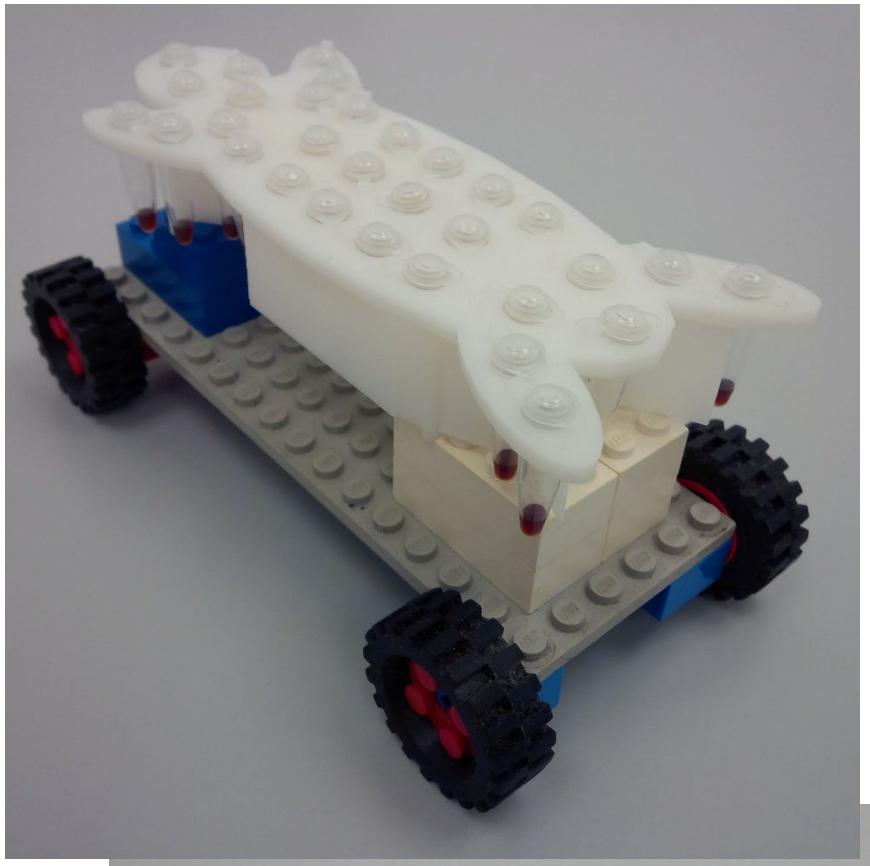

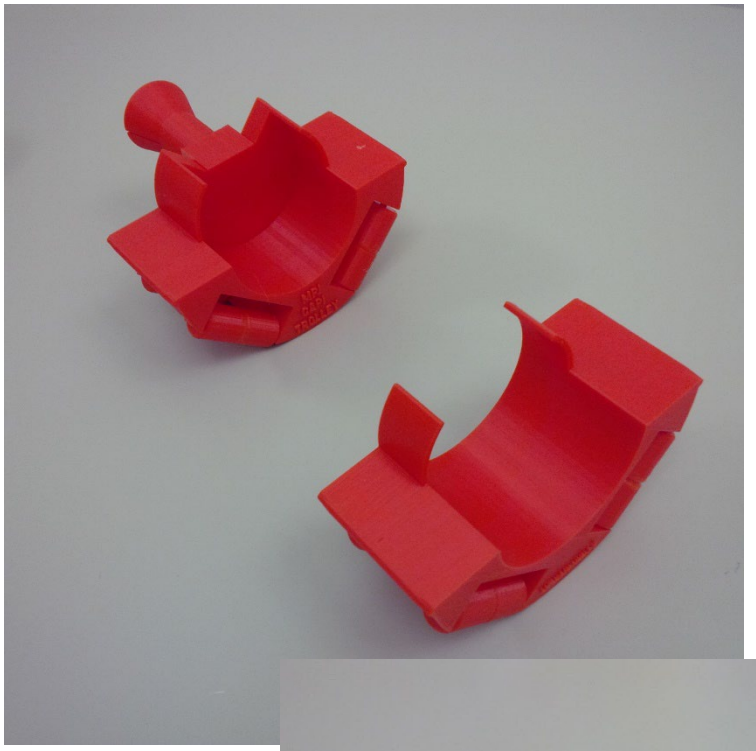

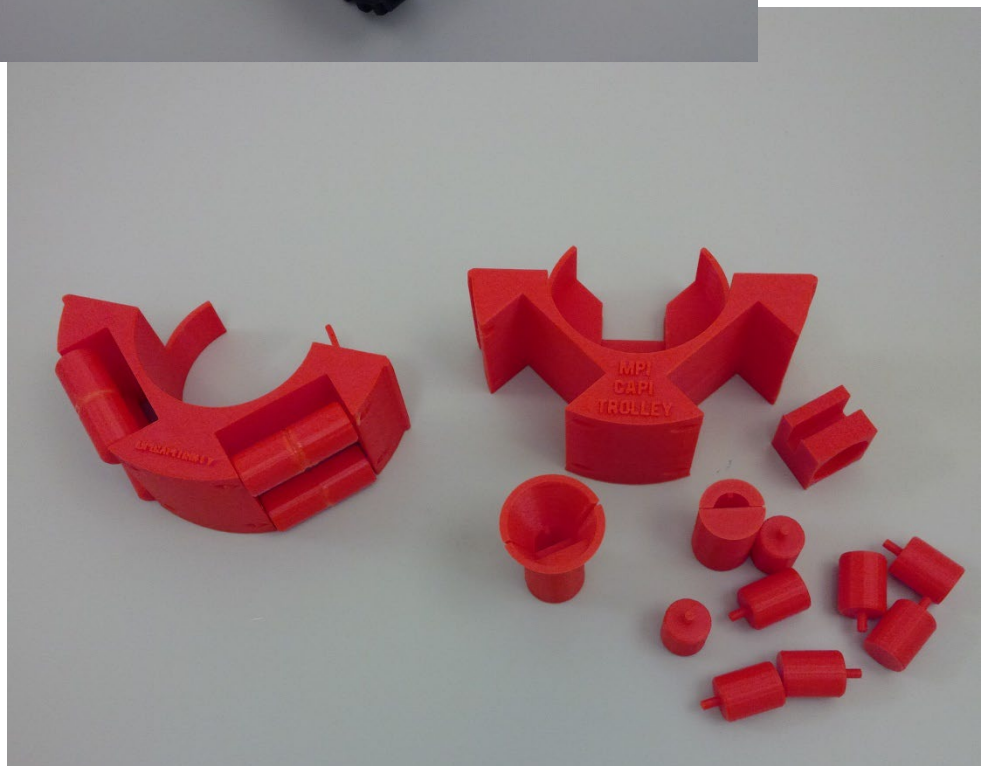
MPI
CAPI
TROLLEY

Scanning volume

Focus field application:

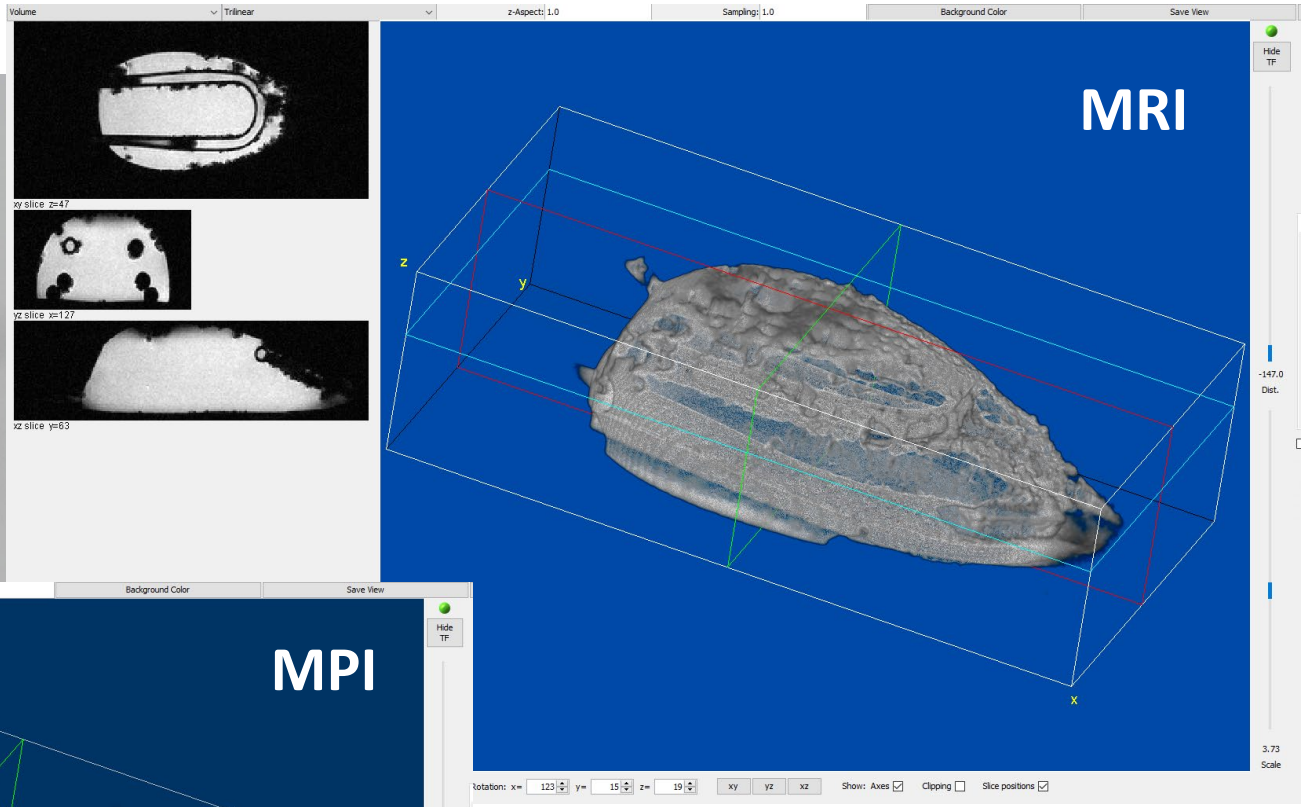

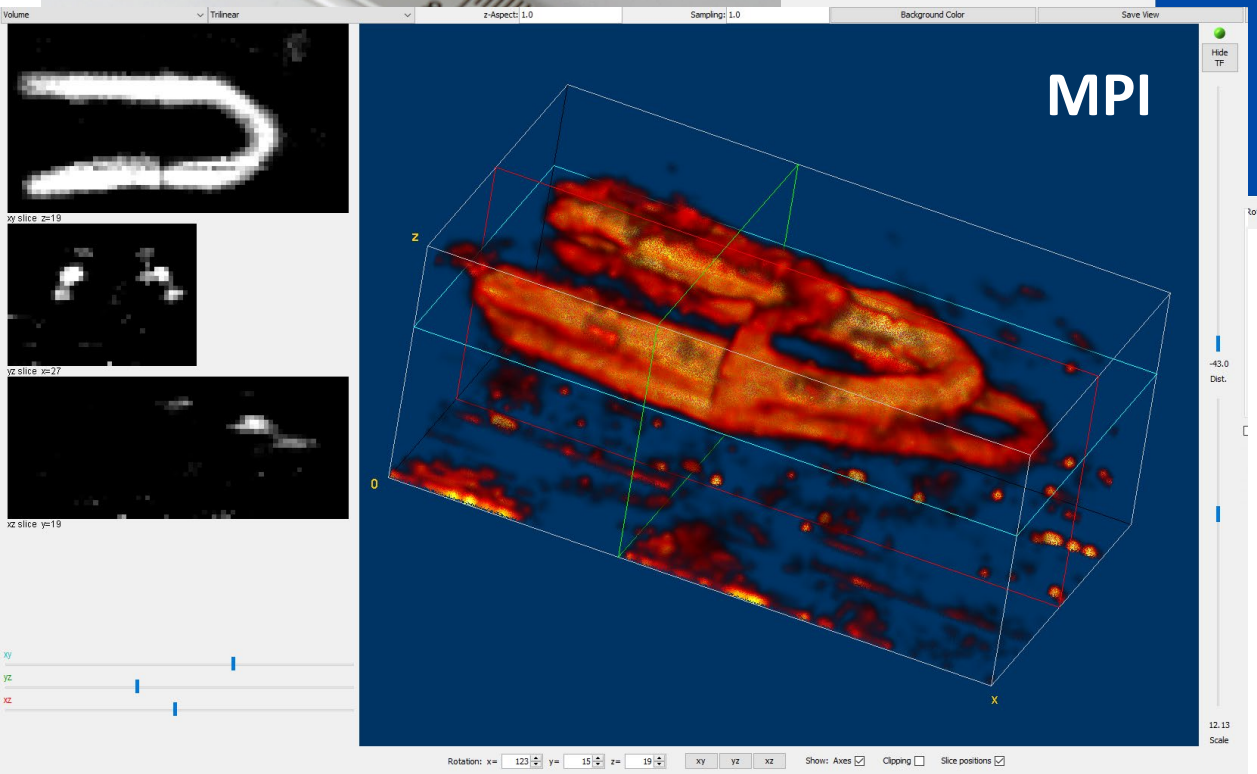

FOV 72 × 40 × 30 mm^3

1 mm resolution

Magnetic nanoparticles in imaging
MRI vs. MPI

MRI: measurement of 1H distribution, signal influenced by nanoparticles

- MPI: measurement directly distribution of magnetic nanoparticles

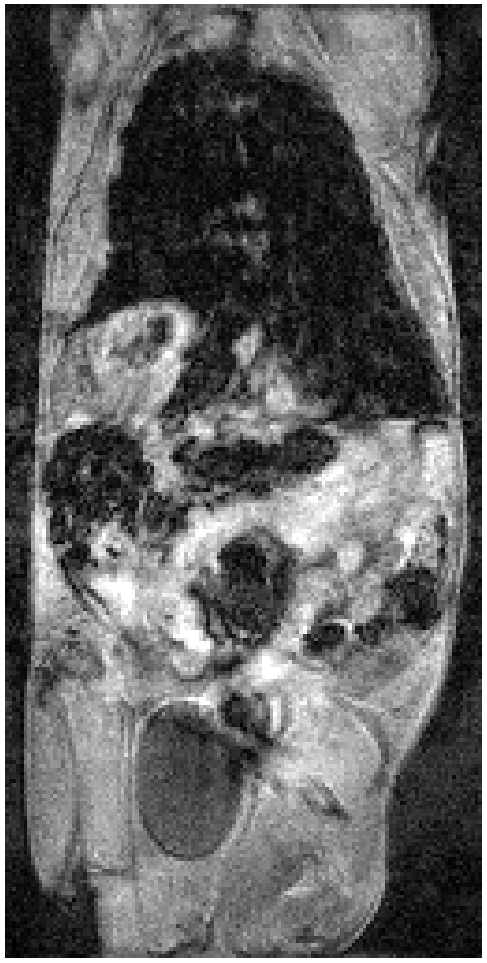

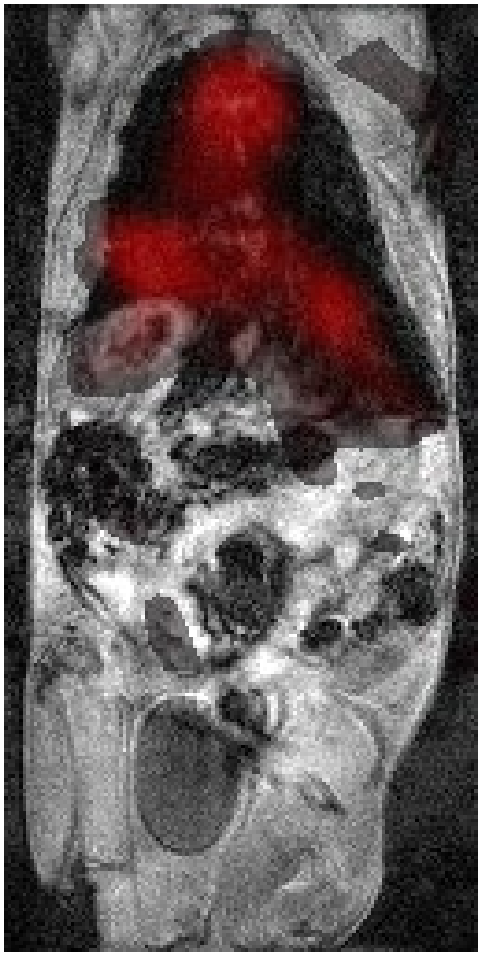

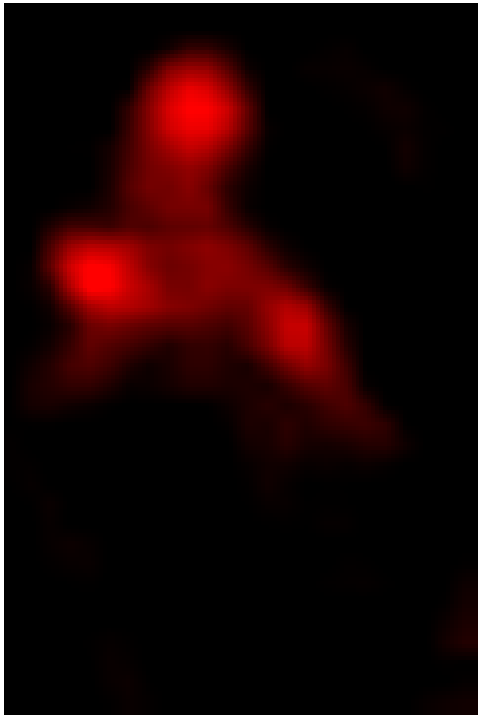

MRI provides anatomical information with an unspecific signal in areas with nanoparticles

MPI provides highly specific information about nanoparticle distribution with no anatomical image

3D reconstruction

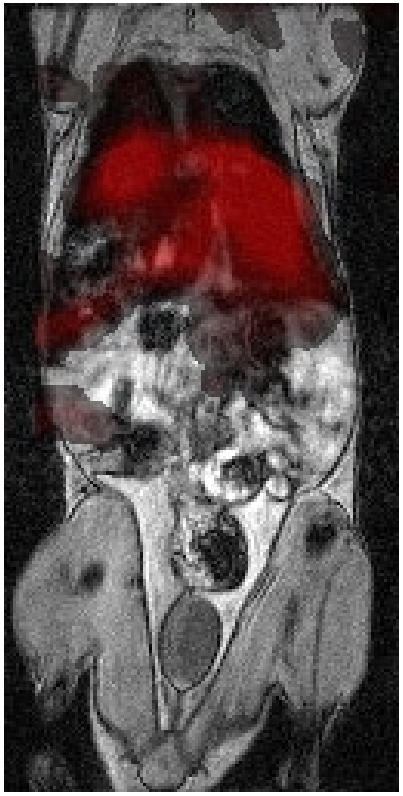

In vivo imaging – nanoparticle distribution

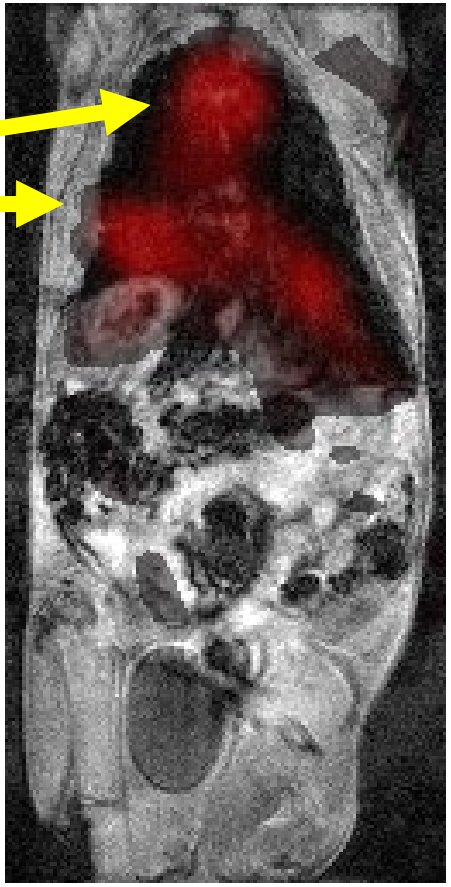

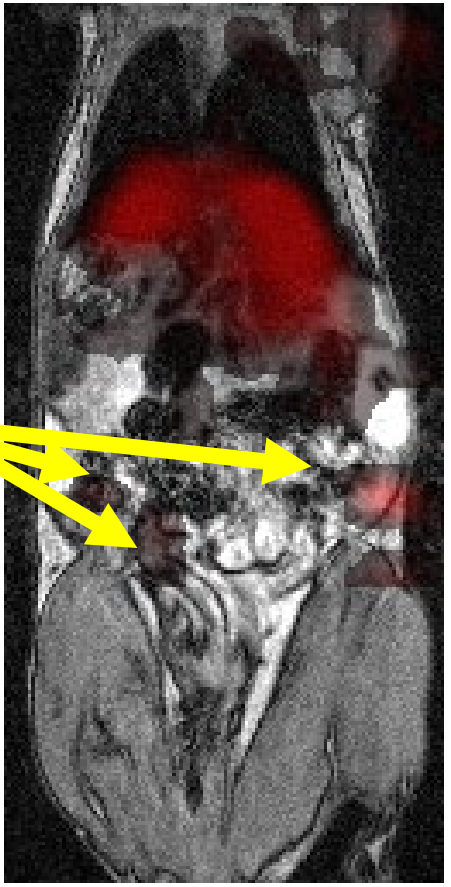

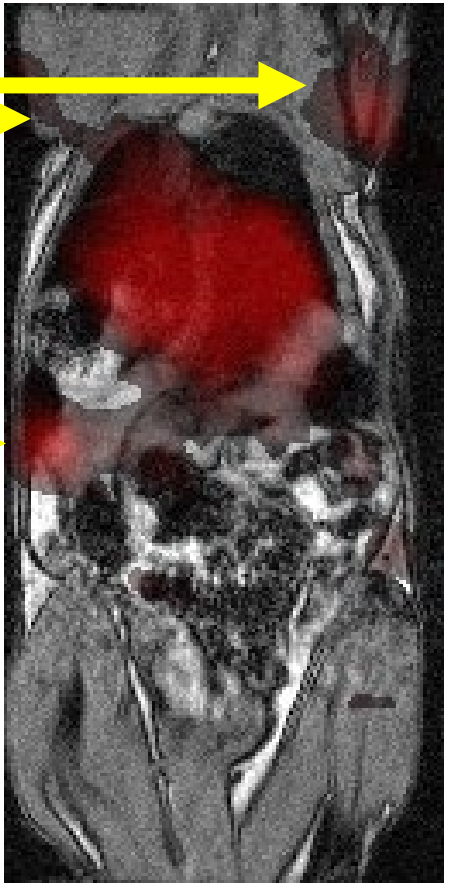

Particle distribution in time

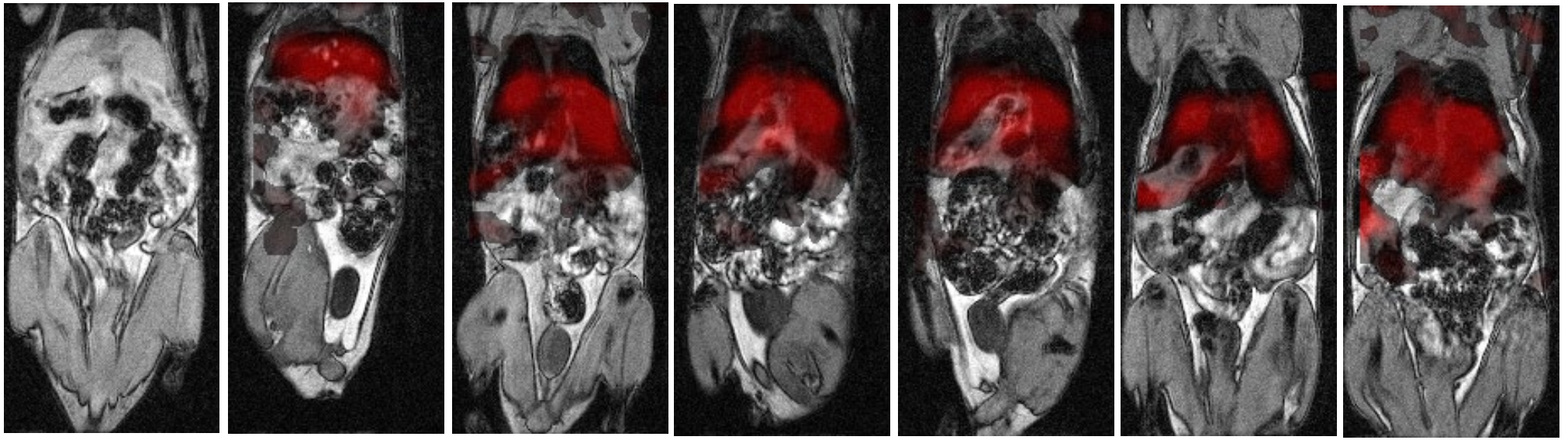

Before app. immediately after 1 day 2 days 7 days 14 days 21 days

Contrast agents - nanoparticles

– Usually iron oxide nanocrystals
– Coated by sugars (dextran etc.) or polymers (poly-L-lysine…), or inorganic compounds (silica)

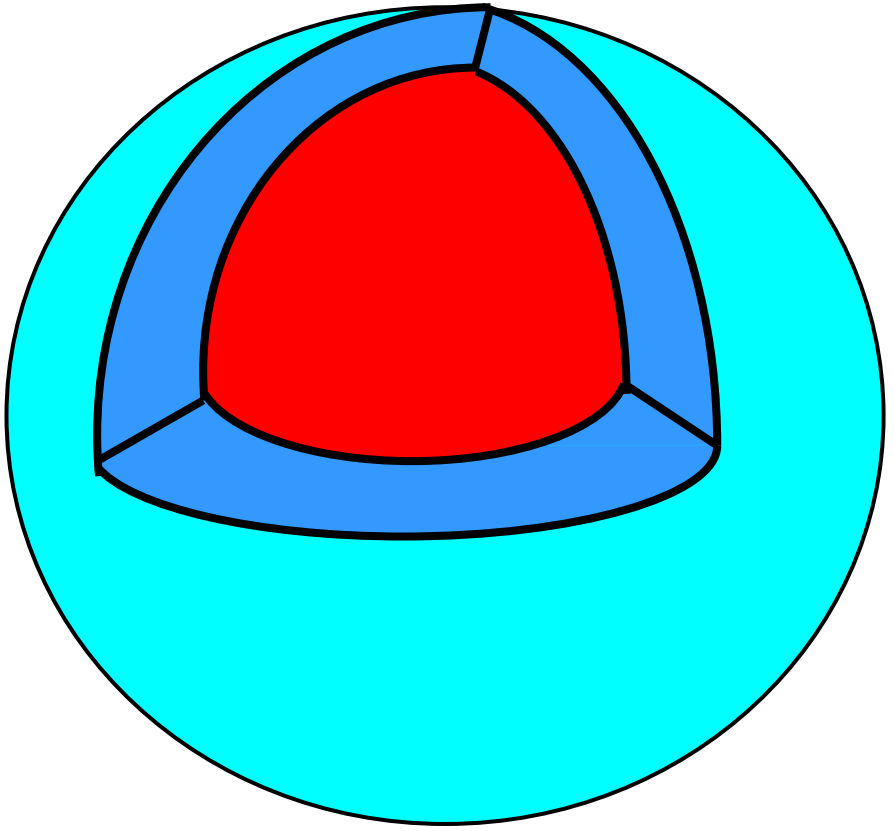

Physical properties define image quality

Nanoparticle relaxation and signal

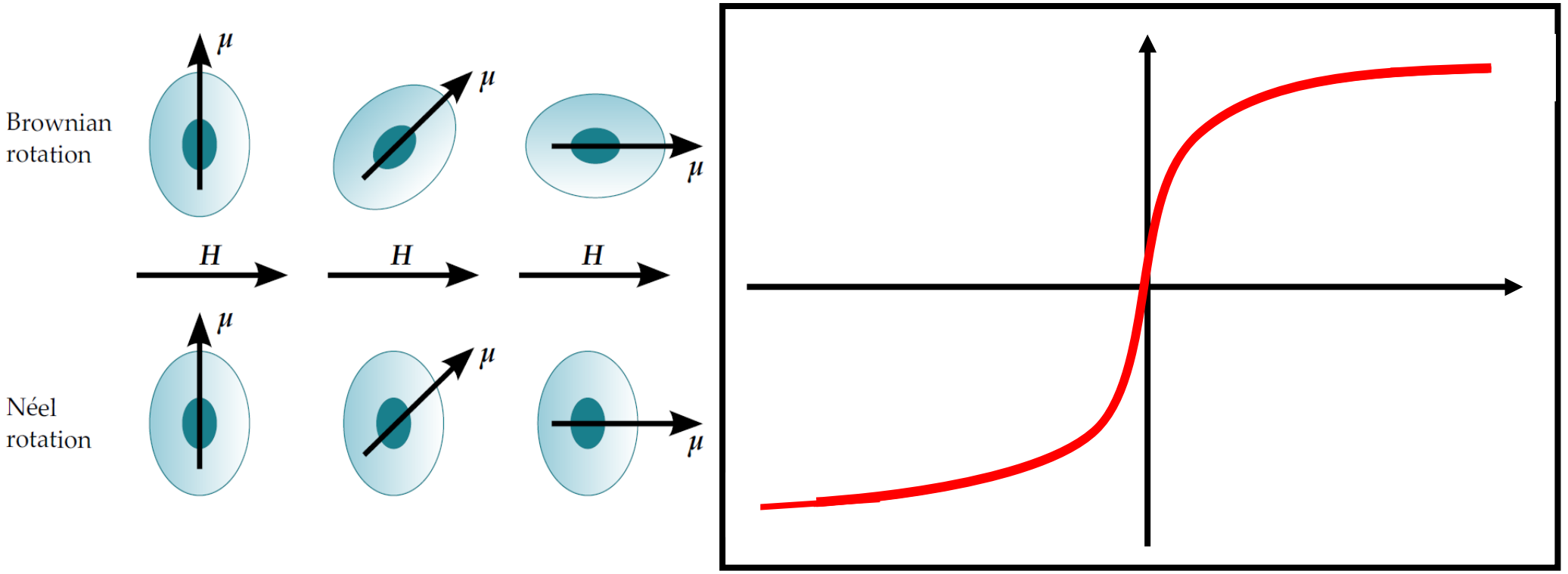

Reorientation is a dynamic process, speed of the response to the external field is crucial

Change of magnetization is effected by

- Néel rotation (change of magnetization due to reorientation of the inner magnetization with respect to the crystal structure
- Brownian rotation (rotation of the whole particle)

Nanoparticle relaxation

Néel rotation is characterized by a relaxation time:

$\tau_N = \tau_0 \exp(K_{eff}\, V / kT)$

K_{eff} magnetic anisotropy energy density
τ_0 corresponds the frequency of gyromagnetic rotation

Brownian rotation

$\tau_B = 3\, \eta\, V_H / kT$

η - viskosity

Both relaxation times are involved in magnetization change
Néel relaxation is faster (in term of orders)

The equations show that the size and shape of particles is important

Nanoparticle relaxation

Combined - efficient relaxation time:

$\tau_{eff} = \tau_{Brown}\, \tau_{Néel} / (\tau_{Brown} + \tau_{Néel})$

1. small particles will most likely exhibit Néel rotation,

2. particles of intermediate volume will perform a combined rotation,

3. large particles will be dominated by the Brownian rotation due to the blocked Néel rotation

The blocking volume / blocking temperature – a crystal critical volume at the given temperature, at which the magnetization is locked during the measuring time (or critical temperature at the given volume)

Nanoparticle relaxation and signal

Why to bother with relaxation?
Why not to just slow down the acquistion if the sample slowly reacts?

Generated signal in the coil ~ electric voltage

$$u(t) = -\mu_0 \int_\Omega \frac{\mathrm{d}}{\mathrm{d}t} \boldsymbol{M}\left(\boldsymbol{H}(\boldsymbol{r},t),\boldsymbol{r},t\right) \boldsymbol{p}(\boldsymbol{r})\, \mathrm{d}^3 r$$

coil sensitivity

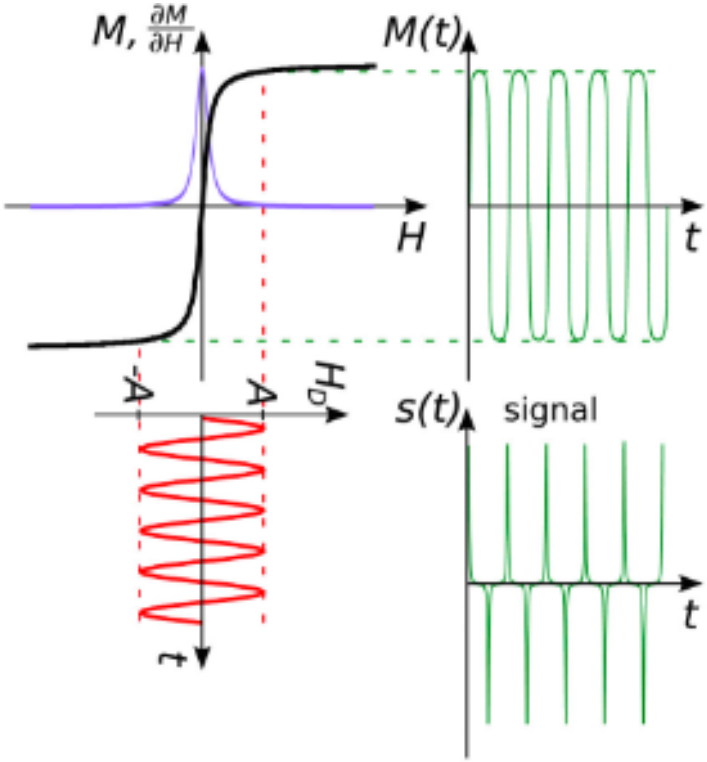

If
- External field is homogeneous in the given volume,
i.e., *p* is constant
- Particle distribution is approximated by δ – distribution…

$$u(t) = -\mu_0 p \frac{\mathrm{d}}{\mathrm{d}t} M\left(H(t)\right)$$

Nanoparticle relaxation and signal

Particles with fast Néel and Brownian relaxations

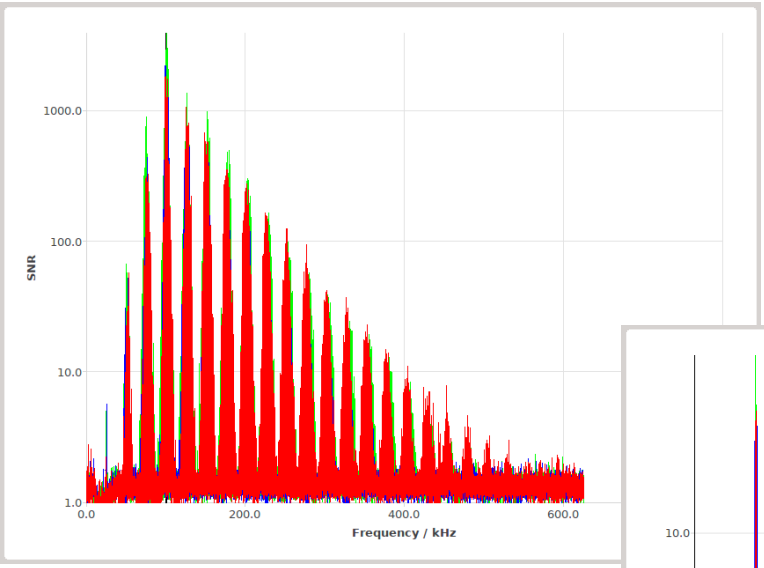

Particles with slow Néel relaxation, and fast Brownian relaxation

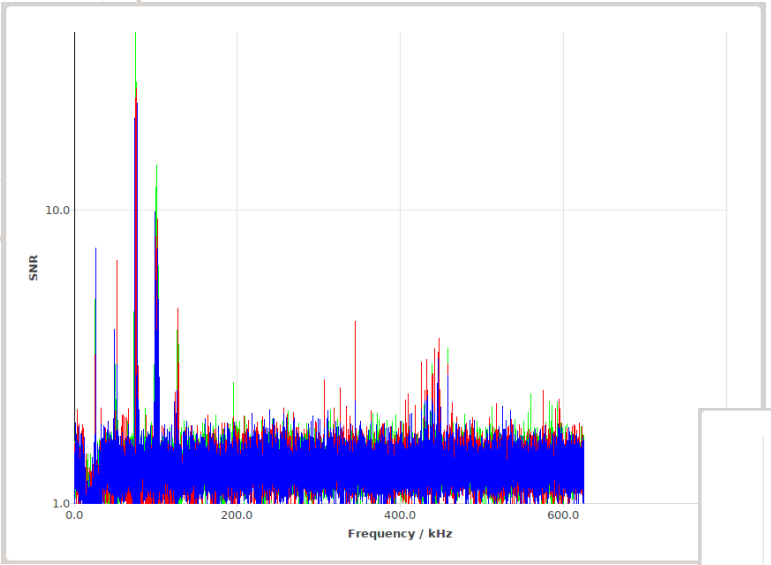

Particles with slow Néel and Brownian relaxations

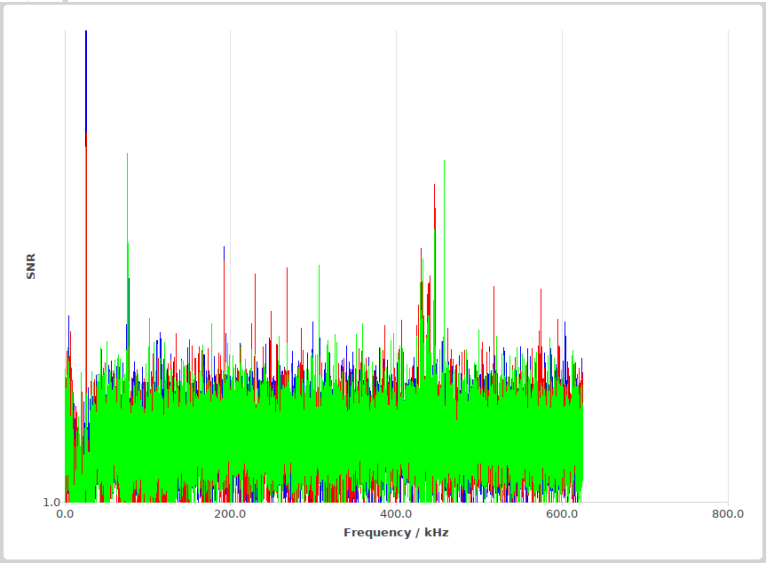

Size and spatial resolution

core size effects the curve through μ

$$M(B) = N\,\mu\,\mathrm{L}(\mu B/kT)$$

The bigger the particles, the higher resolution!

N – number of particles
μ - magnetic moment
B – magnetic induction
k – Boltzman constant
T – tempreature
L – Langevin function, *L* = coth (x) – 1/x

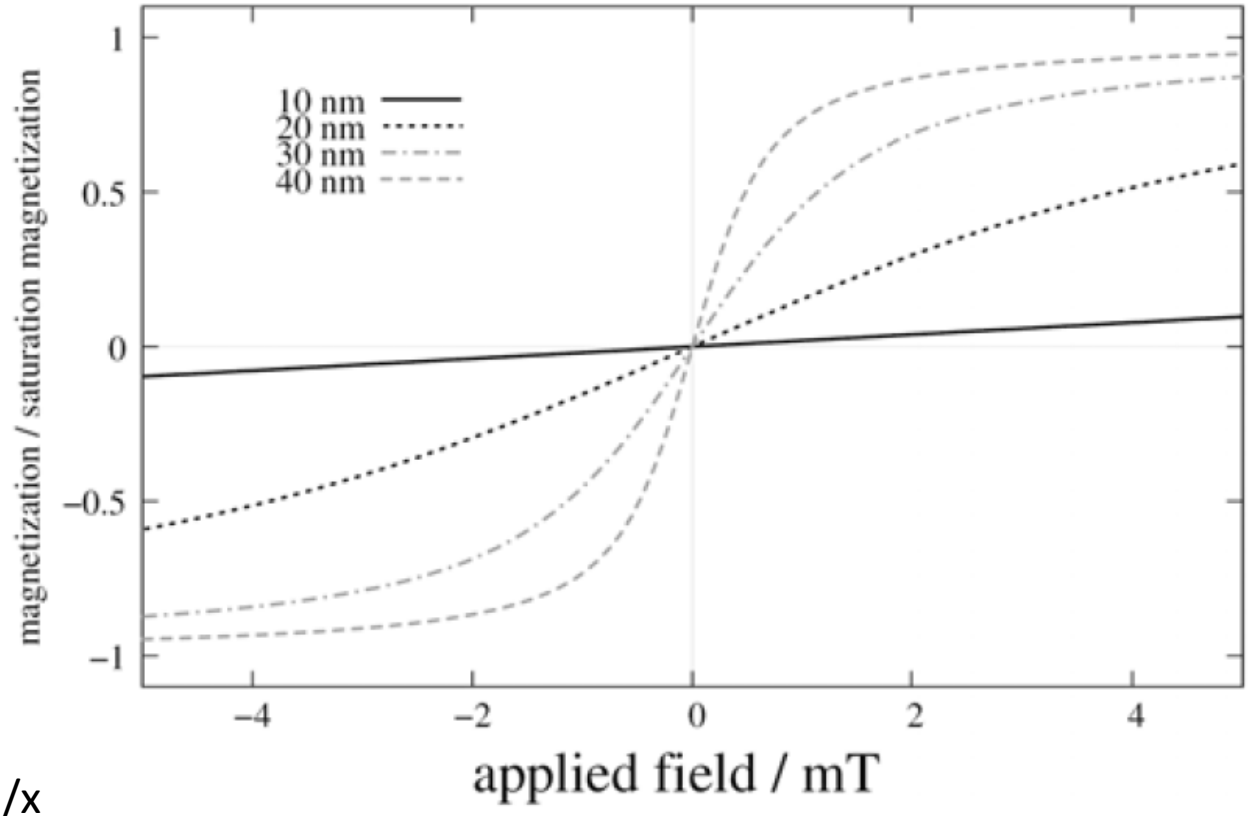

B. Gleich, *Principles and Applications of Magnetic Particle Imaging,*
DOI 10.1007/978-3-658-01961-7, Springer Fachmedien Wiesbaden 2014

Size and spatial resolution

Diameter	saturation field	resolution at $3\,\mathrm{T}\mu_0^{-1}/\mathrm{m}$
10 nm	$31\,\mathrm{mT}\mu_0^{-1}$	21 mm
15 nm	$9.1\,\mathrm{mT}\mu_0^{-1}$	6.1 mm
20 nm	$3.8\,\mathrm{mT}\mu_0^{-1}$	2.5 mm
25 nm	$2.0\,\mathrm{mT}\mu_0^{-1}$	1.3 mm
30 nm	$1.1\,\mathrm{mT}\mu_0^{-1}$	0.7 mm
35 nm	$0.72\,\mathrm{mT}\mu_0^{-1}$	0.5 mm
40 nm	$0.48\,\mathrm{mT}\mu_0^{-1}$	0.3 mm

In real life, we can reach higher resolution by detection of higher number of higher harmonics

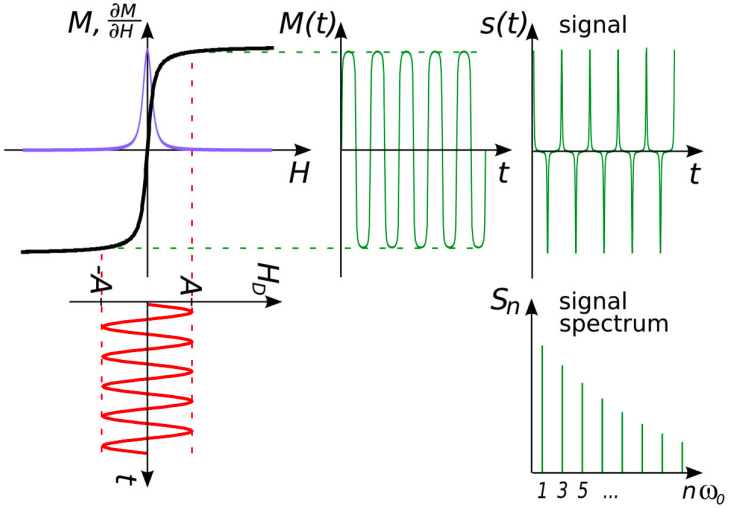

B. Gleich, *Principles and Applications of Magnetic Particle Imaging*, DOI 10.1007/978-3-658-01961-7, Springer Fachmedien Wiesbaden 2014

How the machine looks like…

How the machine looks like…

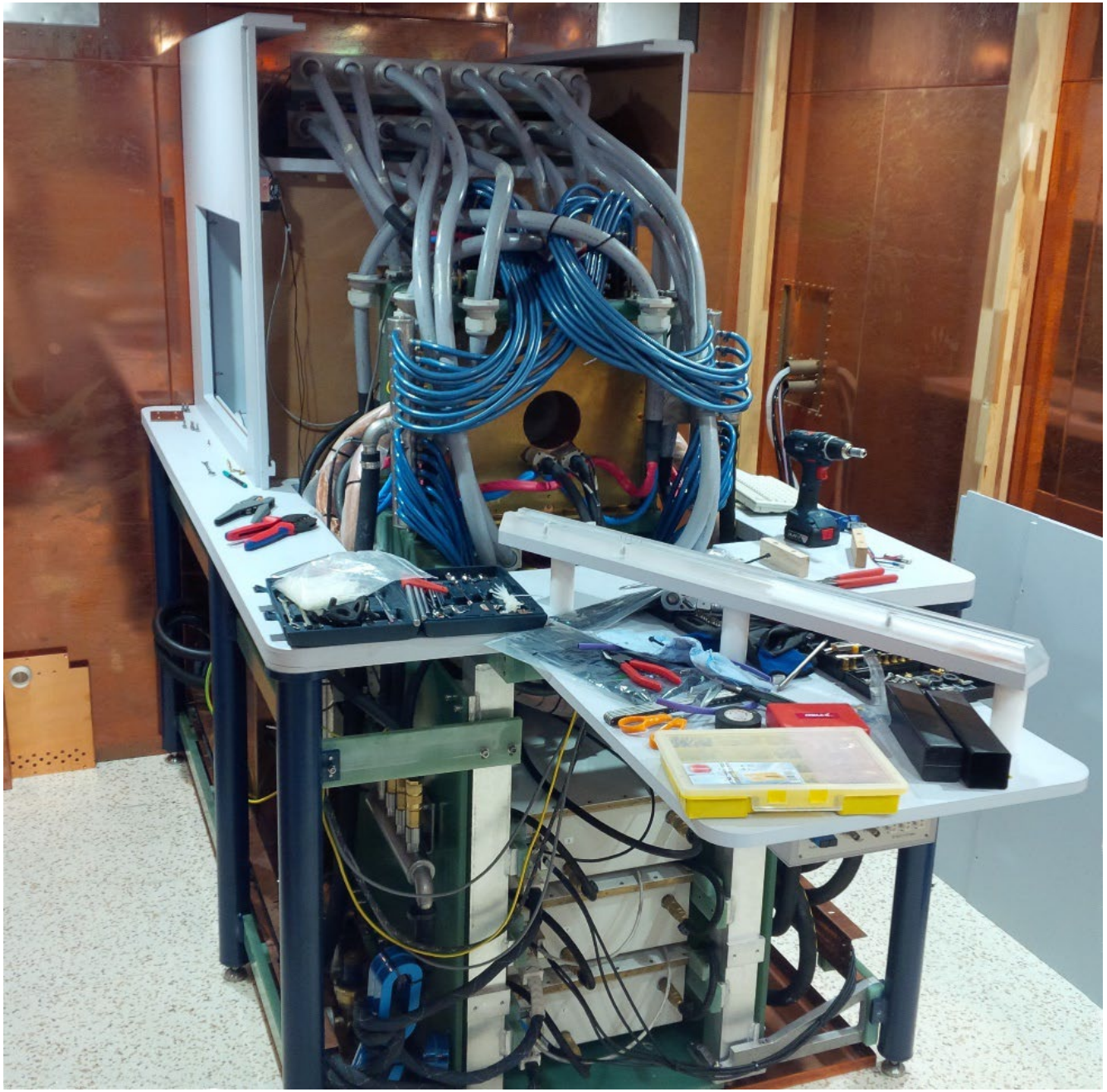

Robot for calibration

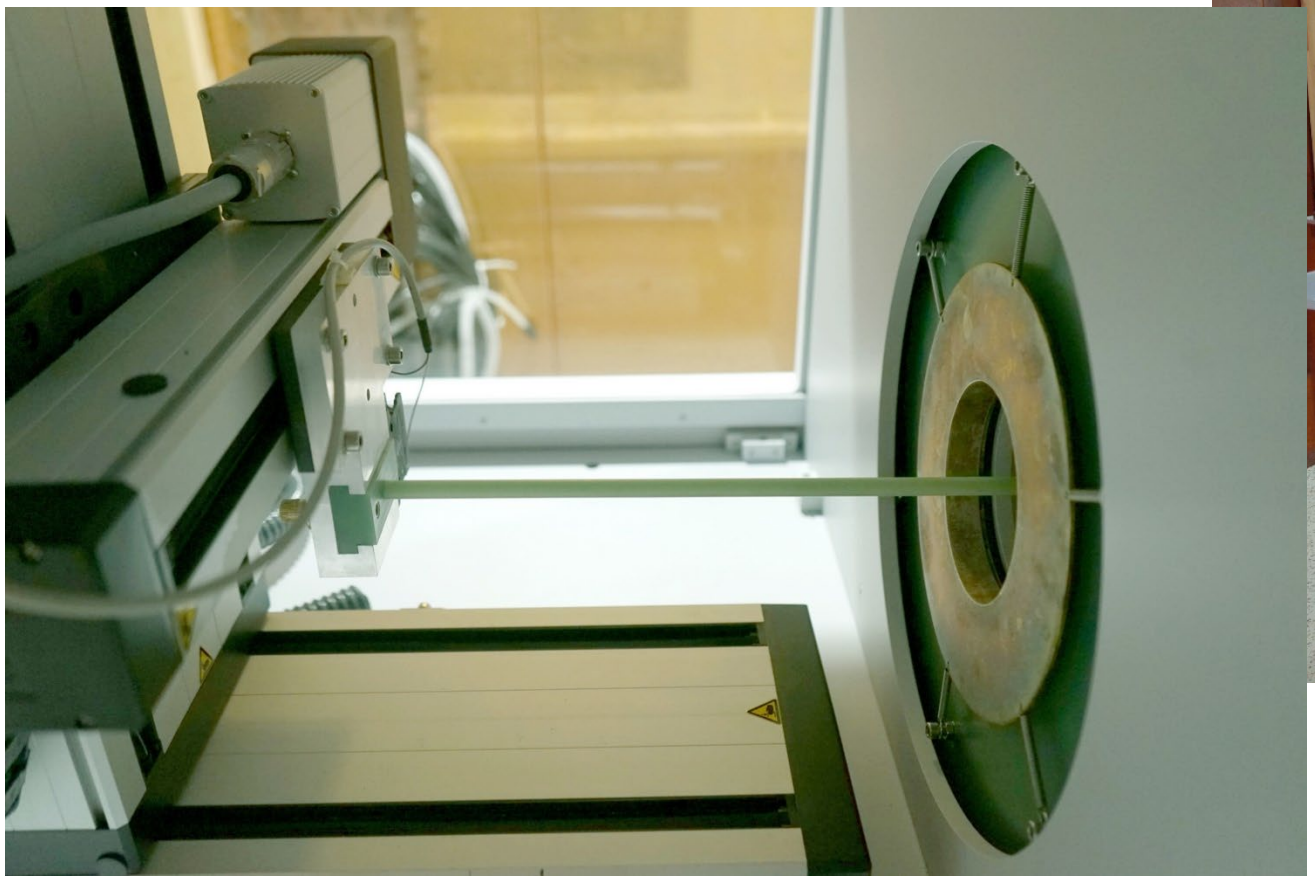

Possible applications

Int J Mag Part Imag

Temperature mapping using MPI

Stroke

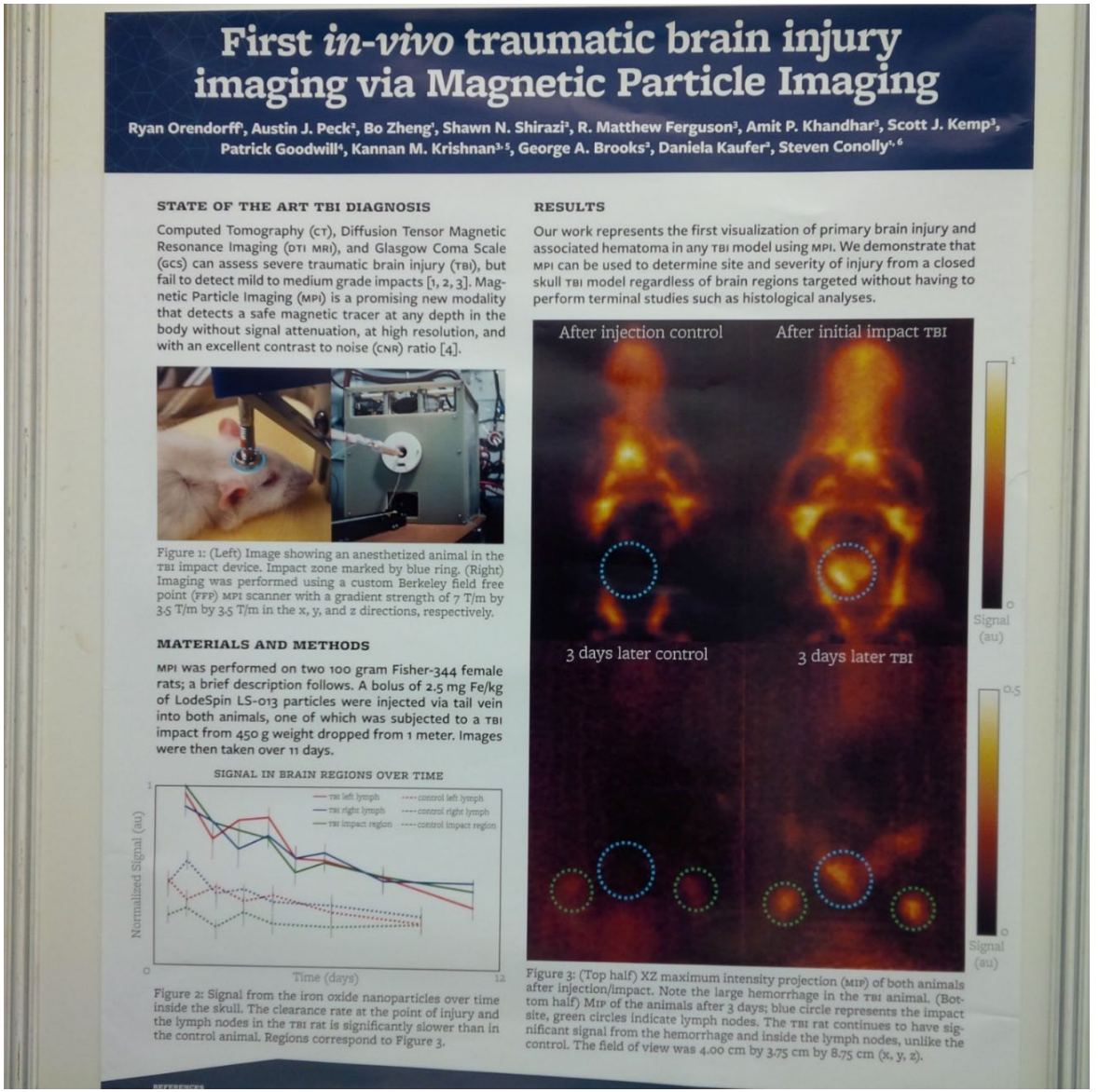

First *in-vivo* traumatic brain injury imaging via Magnetic Particle Imaging

Ryan Orendorff[1], Austin J. Peck[2], Bo Zheng[1], Shawn N. Shirazi[2], R. Matthew Ferguson[3], Amit P. Khandhar[3], Scott J. Kemp[3], Patrick Goodwill[4], Kannan M. Krishnan[3, 5], George A. Brooks[2], Daniela Kaufer[2], Steven Conolly[1, 6]

STATE OF THE ART TBI DIAGNOSIS

Computed Tomography (CT), Diffusion Tensor Magnetic Resonance Imaging (DTI MRI), and Glasgow Coma Scale (GCS) can assess severe traumatic brain injury (TBI), but fail to detect mild to medium grade impacts [1, 2, 3]. Magnetic Particle Imaging (MPI) is a promising new modality that detects a safe magnetic tracer at any depth in the body without signal attenuation, at high resolution, and with an excellent contrast to noise (CNR) ratio [4].

Figure 1: (Left) Image showing an anesthetized animal in the TBI impact device. Impact zone marked by blue ring. (Right) Imaging was performed using a custom Berkeley field free point (FFP) MPI scanner with a gradient strength of 7 T/m by 3.5 T/m by 3.5 T/m in the x, y, and z directions, respectively.

MATERIALS AND METHODS

MPI was performed on two 100 gram Fisher-344 female rats; a brief description follows. A bolus of 2.5 mg Fe/kg of LodeSpin LS-013 particles were injected via tail vein into both animals, one of which was subjected to a TBI impact from 450 g weight dropped from 1 meter. Images were then taken over 11 days.

SIGNAL IN BRAIN REGIONS OVER TIME

Figure 2: Signal from the iron oxide nanoparticles over time inside the skull. The clearance rate at the point of injury and the lymph nodes in the TBI rat is significantly slower than in the control animal. Regions correspond to Figure 3.

RESULTS

Our work represents the first visualization of primary brain injury and associated hematoma in any TBI model using MPI. We demonstrate that MPI can be used to determine site and severity of injury from a closed skull TBI model regardless of brain regions targeted without having to perform terminal studies such as histological analyses.

Figure 3: (Top half) XZ maximum intensity projection (MIP) of both animals after injection/impact. Note the large hemorrhage in the TBI animal. (Bottom half) MIP of the animals after 3 days; blue circle represents the impact site, green circles indicate lymph nodes. The TBI rat continues to have significant signal from the hemorrhage and inside the lymph nodes, unlike the control. The field of view was 4.00 cm by 3.75 cm by 8.75 cm (x, y, z).

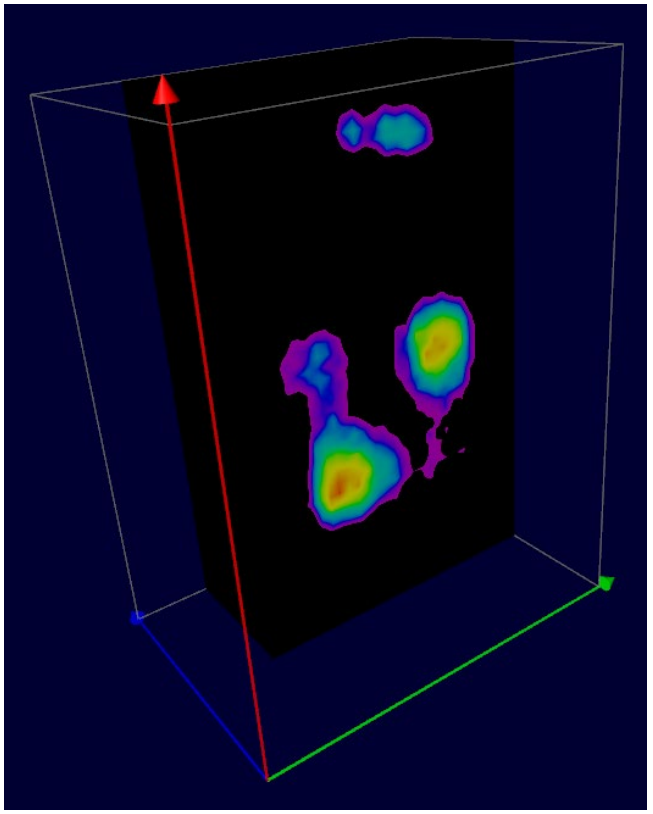

Conclusion

MPI

Potentially interesting imaging method, although its posssibilities are not completely appreciated yet

Requires a contrast agent – only the tracer is imaged

Requires a colocalization with another imaging method

Area for research

- Data acquisition and processing
- Nanoparticle development
- Applications